BIOGENIC SYNTHESIS AND CHARACTERIZATION OF ZnO AND CuO NANOPARTICLES FROM *Entada abyssinica* AND *Warburgia ugandensis* LEAF EXTRACTS FOR ANTI-BACTERIAL APPLICATIONS

BY

LEMEITARON PETER NJENGA

A THESIS SUBMITTED IN PARTIAL FULFILLMENT OF THE REQUIREMENTS FOR THE AWARD OF DEGREE IN MASTER OF SCIENCE CHEMISTRY (ANALYTICAL CHEMISTRY) IN THE DEPARTMENT OF CHEMISTRY AND BIOCHEMISTRY, SCHOOL OF SCIENCE, UNIVERSITY OF ELDORET, KENYA.

SEPTEMBER, 2023

DECLARATION

Declaration by the student

I hereby declare that this thesis is my original work and has not been presented in this University or any other institution for an academic award.

Lemeitaron Peter Njenga

____________________________ ______________________

SSCI/CHE/M/004/20 **Date**

Declaration by the Supervisors

This thesis has been submitted with our approval as the University Supervisors.

____________________________ ______________________

Dr. Kiplagat Ayabei **Date**

Department of Chemistry and Biochemistry,

University of Eldoret, P.O. BOX 1125-30100

Eldoret, Kenya.

____________________________ ______________________

Prof. Teresa Akenga **Date**

Department of Chemistry and Biochemistry,

University of Eldoret, P.O. BOX 1125-30100

Eldoret, Kenya.

____________________________ ______________________

Dr. Zipporah Onyambu **Date**

Department of Chemistry and Biochemistry,

University of Eldoret, P.O. BOX 1125-30100

Eldoret, Kenya.

DEDICATION

This research work is dedicated to my parents, Mr. Lesuno Lemeitaron and Mrs. Rabia Lemeitaron, for their prayers and financial support.

ABSTRACT

In this study, biosynthesis, structural characterizations, optical and bactericidal properties of copper oxide and zinc oxide nanoparticles have been documented. Copper oxide (CuO) and zinc oxide (ZnO) nanoparticles were prepared using *Entada abyssinica* (EA) and *Warburgia ugandensis* (WU) leaf extracts. EA and WU possessed various biomolecules identified in GC-MS and FT-IR analysis which acted as reducing, capping and stabilizing agents in the synthesis of ZnO and CuO nanoparticles. The two-plant species had total phenolic contents, total flavonoid contents and total tannins contents obtained by optical means in the range of 19-58 mg/g, 940-1400 mg/g and 0.6-4.9 mg/g of the acid equivalents, respectively. The total percentage contents of saponins and alkaloids were in the range of 0.94-1.33 % and 1.27-1.42 % respectively. The green route synthesized CuO and ZnO nanoparticles were characterized using UV-VIS (Ultra-Violet Visible Spectroscopy), FTIR (Fourier Transform Infra-red) spectroscopy and X-ray Diffraction (XRD) instrumental methods. The visual observation of color changes during synthesis, the maximum SPR (Surface Plasmon Resonance) peaks observed in the UV-VIS spectra at varied synthesis parameters and the well-developed FT-IR peaks of functional groups responsible for the formation of the nanoparticles confirmed fabrication of nanoscale materials. Time and pH variations were the experimental control parameters. The XRD calculation of average particles sizes confirmed that the synthesized CuO and ZnO NPs were within the nanoscale range. The evaluation of the anti-microbial activities of the biosynthesized nanoparticles against *Escherichia coli* and *Staphylococcus aureus* bacteria was significant since p-value was less than 0.05. In comparison with other test samples against the two bacterial strains selected, the copper oxide nanoparticles synthesized from EA leaf extracts had higher zones of inhibition of 12.0±1.0 mm against *Staphylococcus aureus* pathogen. The lowest inhibition was shown by CuO NPs synthesized using *Warburgia ugandensis* leaf extracts against *Escherichia coli* (7.3±0.6 mm). The research can therefore contribute to the use and documentations of several locally available plants in Kenya in the synthesis of beneficial CuO and ZnO nanoparticles in the treatment of various illnesses.

TABLE OF CONTENTS

LIST OF TABLES

FLOWCHARTS

LIST OF FIGURES

LIST OF ABBREVIATIONS/ACRONYMS

EA- *Entada absyssinica*

WU- *Warburgia ugandensis.*

ZnO - Zinc Oxide

CuO- Copper Oxide

NPs – Nanoparticles

Cu^{2+} - Cupric ion

M- Molarity

eV – Electron Volt

^{o}C – Degree Celsius

UV-VIS - Ultra Violet- Visible Spectroscopy

FTIR - Fourier -Transform -Infrared Spectroscopy

XRD -X-Ray-Diffraction

SPR - Surface Plasmon Resonance

MRSA-Methicillin-Resistant -Staphylococcus -Aureus

ZOI – Zone of Inhibition

CuO NPs – Copper Oxide Nanoparticles

ZnO NPs – Zinc Oxide Nanoparticles

E. coli - *Escherichia coli*

S. aureus - *Staphylococcus aureus*

ACKNOWLEDGEMENT

Thanks to the Almighty God for good health, sufficient grace, strength, guidance and protection during my work. Special regards to my supervisors (Dr. Kiplagat Ayabei, Prof. Teresa Akenga and Dr. Zipporah Onyambu) for their continued support, pieces of advises, words of encouragement and their kindness. Thanks to Mr. Sang' and Mr. Odero; Laboratory technicians in the Chemistry and Biochemistry Department, University of Eldoret for giving me the necessary support and guidance during the laboratory activities.

Thanks to Prof. Martin Onani, University of Western Cape, South Africa for assisting in the analysis of samples for XRD. God bless you abundantly. I wish to thank the Department of Chemistry (JKUAT), for the facilitation of UV-VIS and FTIR analysis. I sincerely thank John Lemuna, Betty Gitonga, Ann Osborne, Annier Hinoh and County Government of Laikipia and Samburu, for their financial support throughout the study. Thanks to my parents, sisters and brothers for their prayers and their unending love.

CHAPTER ONE

INTRODUCTION

1.1 Background of the study

Nanotechnology has greatly developed and has led to wide production of nanoparticles that are medically used in therapy, monitoring, diagnosis and detection. Nevertheless, inorganically synthesized nanoparticles by conventional techniques (solvothermal and hydrothermal), are not economical due to low bioavailability, poor targeting and poor biocompatibility (Yao *et al*., 2021). Nanoparticles are defined as molecular or atomic solid particles in the nanometer scale (1-100 nm) and possess excellent properties unlike wholescale molecules when comparing their morphology and sizes. Metal and metal oxide nano-sized particles have been carefully studied in nanotechnology and science because of their outstanding properties like high dispersion and volume to surface ratio in solution. These metal oxide and the metal nanoparticles show great anti-bacterial potentials (Vanlalveni et al., 2021). The surface atoms percentages become very important. This unique shape and size-dependent property has led to its extensive application commercially (Tee & Ye, 2021).

In nanotechnology, various plants have been used to synthesis metal oxide nanoparticles like *C. fistula* and *M. azadarach.* The biogenically fabricated nanoparticles displayed positive antibacterial activity towards the microorganisms in comparison with standard medicines, signifying that plant-mediated synthesis of nanomaterials is an outstanding method to come up with environmentally friendly and useful medicinal products (Naseer *et al*., 2020). *Aloe barbadensis* was also applied in the biosynthesis of CuO NPs (Batool & Mehboob, 2018).

The search for biologically artificial friendly approaches has reduced worries by forcing inventors towards bioinspired synthesis which is both green and economical. Nanoparticles synthesis using numerous chemical and physical procedures has shown drawbacks like the practice use of high temperature action, high costs, application of toxic and harmful reagents, use of classy equipment and high energy thus disastrous to the atmosphere*(*Khodadadi *et al*., 2021*)*.

In green synthesis, the biomolecules from plants powerfully bind and enclose the surfaces of nanoparticles. The extracts possess several bioactive compounds namely; phenols, tannins, proteins, flavonoids and terpenoids. The metabolites take significant part to reduce and stabilize the metal salts to form nanoparticles (Waris *et al*., 2021). The nanomaterials will possess properties of phytochemicals and nanoparticles (George *et al*., 2021). The plant extracts are mixed with the metal salts at temperatures less than 100 ^{o}C for a specified duration.

In addition, bio-synthesis of nanoparticles from metals has several benefits of being faster, non-toxic, easier to produce, use of in-expensive chemicals, environmentally friendly and controlled shapes and sizes. The chemical and physical synthesis techniques have numerous limitations and possible problems. The toxicity of chemically synthesized nanomaterials restricts the application in medicine and biology *(*Khatamifar & Fatemi, 2021).

Table 1.1 and figure 1.1 illustrates the biosynthesis methods of metal oxide nanoparticles in a simplified way**.**

Table 1.1: The effectiveness of plant-mediated synthesis techniques compared to chemical and physical routes

NO	**CHEMICAL/PHYSICAL TECHNIQUES**	**BIOSYNTHESIS**	**REFERENCES**
1	Low production rate and costly	Eco-friendly in nature, low costs	(Akbar *et al*., 2020)
3	Use of harmful chemicals	Application of less-toxic chemicals	(*Ahmad & Kalra, 2020*)
4	Environmental pollution and large-scale production results to high expenses	Facile	(Algebaly *et al*., 2020)
5	High temperature dependent reaction rates	Low temp, simplicity and fast.	(Rangel *et al*., 2020)
6	High pressure, radiations, expensive, toxic, difficult to operate	Abundant availability and environmentally fit	(Perveen *et al*., 2020)
7	High associated costs, limited to high pressure and temperature and time-consuming.	No use of specialized and complex procedures like multiple purification steps, culture maintenance and isolation.	(Garibo *et al*., 2020)

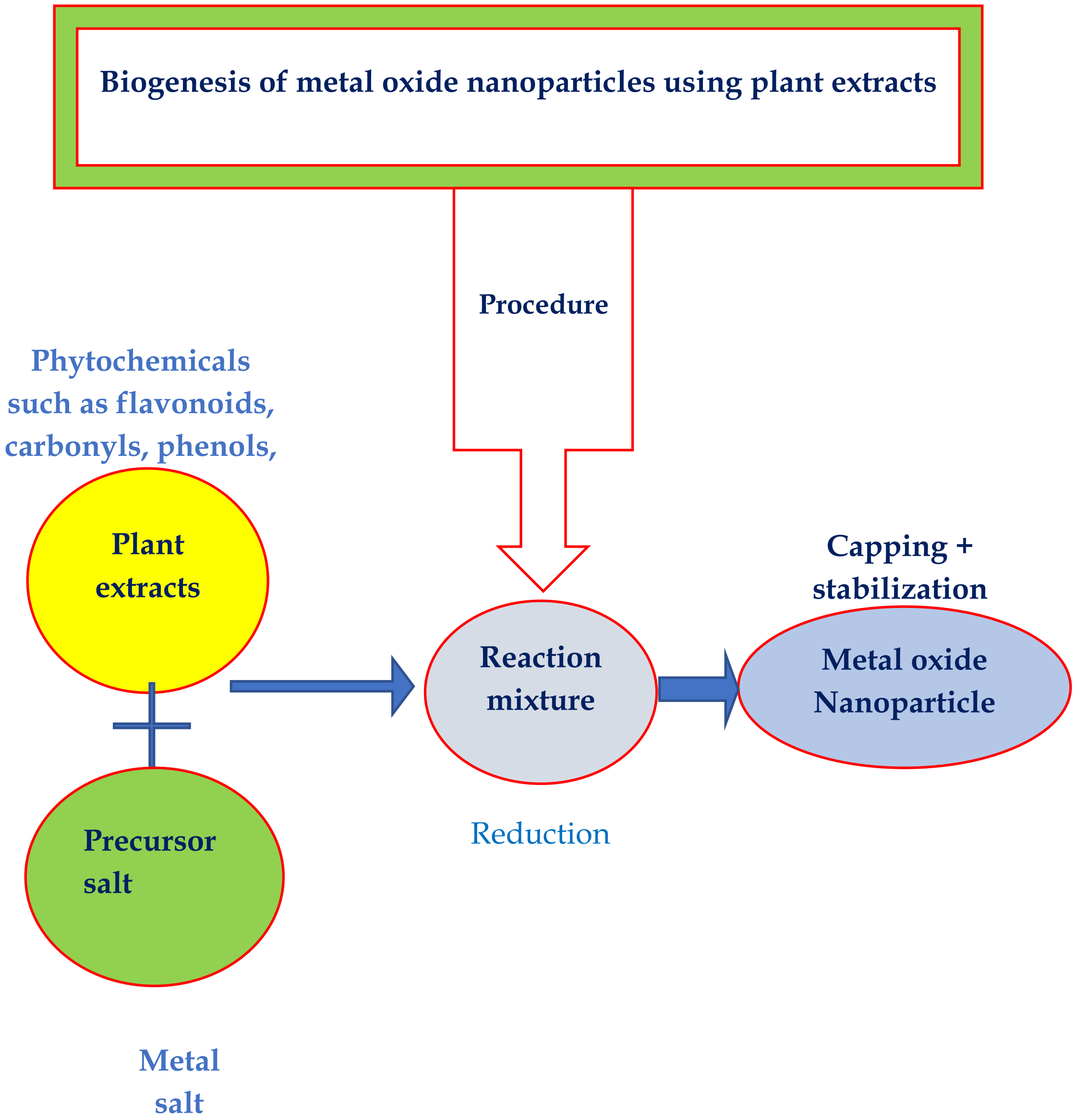

Figure 1.1: The bioinspired synthesis mechanism of zinc oxide and copper oxide nanomaterials

Microorganisms established resistance against drugs like linezolid, dyad, daptomycin and dalfopristin. Therefore, the requirement for novel compounds is enormous. Natural products are in the lead of study as demonstrated by isolating teixobactin and darobactin. This is because these components are in plants are active components that are anti-microbial (Biegański *et al.*, 2021).

Medicinal plants play a vital part in sustaining the health of humans as well as enlightening their quality-of-life for many years. They have been utilized to effectively treat many sicknesses due to possession of compounds that have reducing capability known as antioxidants (Dayana *et al.*, 2021). According to Kenya's reported data of 14 public hospitals by *(*Maina *et al.*, 2020*)*, about one percent of the in-patients were diagnosed against bacteria or microbials. It was noticed that the most affected were the adults in all the five named departments (medical, neonatal, pediatric, surgical and surgical-pediatric). Many communities valued the application of medicinal plants in treatment of both livestock and human sicknesses. Plants possess many different phytoconstituents with pharmacologic potentials. The phytoconstituents (hydrocarbons, phenols, flavonoids, saponins etc.) can be extracted locally in preparation of herbal medicines. It was estimated by World Health Organization (WHO) that about 80% population in the world depends mainly on herbal-medicines prepared in primary treatments in health services especially middle and low income countries (Obakiro, Kiprop, Kigondu, K'Owino, *et al*., 2021).

The antimicrobial activities of the bioinspired synthesized nanoparticles in metal oxide form is well known. They result to the death of the microbes by penetrating through easily the cell membranes and distorting them (Joshi, 2020). The development in biomedical applications involved functionalized, bio-degradable and biocompatible nanoparticles and it is currently a vibrant and marvelous part to investigate. The other bio-medical applications being well researched on are quantum dots, paramagnetic, carbon nano-tubes and nano-shells. The examples of nanostructures include zinc, copper and silver oxide nanoparticles *(*Kalpana & Devi Rajeswari, 2018).

The main goal of the research was to biogenically synthesize zinc oxide and copper oxide nanoparticles from *Entada abyssinica* (EA) and *Warburgia ugandensis* (WU) leaf extracts. It also pursued the characterization of the nanoparticles using UV-V*I*S, FT-*I*R and X*R*D instrum*e*ntation techn*i*ques. The nanoparticles were t*e*sted and compar*e*d for their bactericidal pot*e*ntials aga*i*nst *Escherichia coli* and *Staphylococcus aureus* bacterial strains. Therefore, the aim of this study was to encourage and promote the use of these eco-friendly approaches of using traditionally medicinal valued plants in medical practices to treat the various life-threatening microbial illnesses in the 21st century.

In the past 2 decades, the research on natural products has immensely increased worldwide. This has been contributed to the increased number of cases of decreased chemically diversified libraries of natural products, rise of new illnesses and resistant microbes. These scientific searches are to make an extra effort to develop a substitute for prescribed medicines that are expensive and come up with therapeutic agents that are cheap, safe and most effective (Obakiro, Kiprop, Kigondu, K'Owino, *et al*., 2021).

1.2 Statement of the problem

Bacterial diseases like typhoid, cholera, strep throat and many others are the main bacterial infections caused and account much infections in health sector in Kenya. It is a significant cause of mortality in immune susceptible individuals like cancer and diabetic persons.

In addition, the development of drug resistant bacterial pathogens, has become a major problem in health sector necessitating further research to come up with new drugs. Thus, green synthesis is a promising approach towards developing new drugs and curb anti-microbial resistance**.**

The invention of antibiotics has really increased the superiority of life of many humans in the universe seeking medical services. The drug resistance by most microbes has been resulted by misapplication and over-usage of anti-biotics rendering them less effective. This is posing a great risk in the curing of microbial illnesses due to the continued trend of misappropriation of these drugs. It needs to be attended to as a significant concern to reduce development of resistant bacteria towards drugs *(*Hu *et al., 2021).*

The prescribed antibiotics in primary care is about 80% and great efforts are made to avoid unnecessary applications. Urgent action is required to reduce deaths caused by drug resistant microbes. Globally, 700 thousand deaths (per year) were reported by health ministers (G20) and predicted that by 2050 to be over ten million (Gulliford *et al.*, 2020). The SBI (Serious bacterial infection) like fever, has immerged from over-use of anti-biotics causing a great concern to pediatrician treating and parents. The disease has become a leading cause in hospital admissions and medical consultations in children (Pathak *et al*., 2020). It is therefore important to apply the field of nanotechnology in research to come up with nanoparticles that possess anti-bacterial and anti-cancer activities by using plant extracts of various selected medicinal plants. In this research, WU and EA was explored in the synthesis of nanomaterials for anti-bacterial tests.

1.3 Significance of the study

The green synthesis and application of metal oxide nanoparticles such as ZnO and CuO NPs in medicine in the treatment of bacterial, fungal and tumors has been studied (Datta *et al*., 2017), (Awwad *et al*., 2020). This is because it has been proven that medicinal plants are highly cost effective unlike chemical methods that are highly unfriendly due to toxicity of the applied chemicals and conditions involved such as high temperatures and pressures. The plants are rich in phytoconstituents such as flavonoids, alkaloids, polyphenols and phenols identified through phytochemical screening which are responsible for capping and stabilization of the nanoparticles of interest.

The biosynthesized nanomaterials are applied in anti-bacterial properties due to their small sizes and shapes that make them effective to penetrate through the cell membranes of microbes, inhibit cell division and cause death. Therefore, there is a need to venture into the research of synthesis and application of nanoparticles in medicine due to the prevalent bacterial diseases due to the current existence of multi-drug resistant bacteria.

Medicinal plants in Kenya are believed to be highly effective since they have been used by local communities in the treatment of various illnesses. The obtained results from the study inspire the formulation of new anti-bacterial drugs to treat various bacterial diseases.

The results obtained can assist get rid of MDR (Multi Drug Resistant) microbes towards commonly used antibiotics.

The study also reveals the presence of various important biomolecules that are important in the synthesis of metal oxide nanoparticles and also their applications in herbal treatment of diseases. The study supports the application of the biosynthesized nanoparticles in bactericidal activities, antioxidant and photocatalysis activities. The study will also trigger the most cost effective, environmentally friendly and stable technique of synthesizing nanostructures that replaces chemical and physical methods that are harmful due to application of harmful chemical reagents.

1.4 Objectives

1.4.1 General objective

To synthesize copper oxide and zinc oxide nanoparticles from *Entada* abyssinica and *Warburgia ugandensis* leaf extracts and evaluate their individual bactericidal activities.

1.4.2 Specific objectives

i. To qualitatively and quantitatively determine phytochemicals, present in *Entada abyssinica* and *Warburgia ugandensis* leaf extracts.

ii. To synthesize copper oxide and zinc oxide nanoparticles from *Entada abyssinica* and *Warburgia ugandensis* leaf extracts.

iii. To characterize the green synthesized nanoparticles using XRD, UV-VIS and FT-IR instrumental methodologies.

iv. To evaluate and compare efficacy of the nanoparticles against selected bacterial strains (*Escherichia coli* and *Staphylococcus aureus*).

1.5 Research questions

i. Which phytochemicals are present in *Entada abyssinica* and *Warburgia ugandensis* extracts?

ii. Can the extracts of *Entada abyssinica* and *Warburgia ugandensis* synthesize copper oxide and zinc oxide nanoparticles?

iii. What is the crystallinity structure and average particle sizes of the green synthesized copper oxide and zinc oxide nanoparticles?

iv. Is there any effective bio-activity against the selected bacterial pathogens by the green synthesized copper oxide and zinc oxide nanoparticles?

CHAPTER TWO

LITERATURE REVIEW

2.1 Green synthesis of nanomaterials/nanoparticles

The term “Green-Synthesis” is a bottom-up approach that refers to the application of environmentally friendly materials that are compatible to bio-medical and pharmaceutical uses. There are no harmful reagents used during the fabrication (synthesis) processes. It is also termed as a biological process because the synthetic process involves use of plants, bacteria, fungi or algae. Green synthesis is recommended because it is cost-effective, energy saving and a greener approach (Mutukwa & Taziwa, 2022).

Zsigmondy Adolf Richard was named the first to describe nm (nanometer scale). Richard Feynman Laureate (a Nobel Prize and American physicist) during a certain yearly society gathering of Physical America gave a speech in 1959. It was purely academic and it was rated the first talk on nanotechnology. The lecture presented was highlighted as; “At the Bottom, Plenty of Room Is Available. ‘’ During this meeting, the following concept was presented; ‘‘why can’t we write the entire 24 volumes of the Encyclopedia Britannica on the head of a pin?’’ The vision was to develop smaller machines, down to the molecular level.’’ (Baig *et al*., 2021).

Nanotechnology regulates nanoparticles in the range of 1-100 nm. The nanoparticles have diverse properties compared to great particles such as small size, possible use in catalysis, chemical reactivity, distribution and unique such as zinc oxide. Zinc oxide is considered a harmless compound in Drug Administration and Food by U.S *(*El-Hawwary *et al*., 2021). Nanomaterials of zinc oxide also possess incredible and extraordinary photocatalytic (photodegradation of dyes), antioxidant and antibacterial activities because they have large surface area (Garg, 2021). Plant components such as starch is considered to be the greatest stabilizing mediator that is biocompatible, renewable and abundant in the synthesis of metal oxide nanoparticles such as copper oxide. This biopolymer cooperates with the surfaces of nanoparticles because of the possession of hydroxyl groups (Jiménez-Rodríguez *et al*., 2021).

The green synthesized metal oxide nanoparticles such as copper oxide, silver oxide and zinc oxide, have inspiring physical and chemical properties such as neutral pH, longer shelf life, UV radiation absorption, multifunctional, promising and strategic inorganic materials. They have multiple application zones such as solar energy translation, piezo-electricity, electrical, photosensitivity, semi-conductivity and chemical sensitivity. They have great exterior area leading to enlarged catalytic and chemical reactivity (Gunathilaka *et al*., 2021). During the green synthesis processes, gold and silver nanoparticles are comparable according to activity processes but silver nanocomposites are cheap to handle. The catalytic processes of silver (Ag) are popular at asymmetric aldol reactivities, C-C activations and C-H activations due to higher enantioselectivity and regioselectivity towards the formation of products. Silver (I) complexes are much applied in C-C activation especially for nucleophilic reactions because of its p-Lewis acidity property (P. Singh *et al.*, 2020).

The changes in colour during the green synthesis of the plant-mediated nanoparticles was reported by Naseer *et al*. In order to obtain small sized nanomaterials, temperature was importantly considered as a contributive factor. Therefore, the smaller sizes of nanoparticles depended on higher temperatures during the reaction of the mixtures between the plant extracts and the precursors (metal salts). A relative temperature between 60-80 °C is considered appropriate in incubating reactants leading in the fabrication of the zinc oxide nanoparticles that are very small-sized (Naseer *et al*., 2020).

Several methodologies such as thermal disintegration, hydrothermal, chemical reduction, electro-reduction and electrochemical have been established to prepare nanomaterials such as copper oxide nanoparticles. The researchers have recently based on scientific study of synthesizing nanoparticles via green routes using flowers, bark and leaves extracts (Amer & Awwad, 2021).

The biogenic synthesis of nanoparticles is well documented (**figure 2.1).** This mechanism undergoes three significant steps: (i) the activation step that involves the nucleation of the reduced metal atoms by phytochemicals in plant extracts from metal cations resulting to metabolic complexes and metal ions. (ii) Growth stage also called Ostwald ripening that causes increased nanomaterials' thermodynamic stability as a result of reduction of metal cations and spontaneous agglomeration of small nanoscale particles to large size particles. This is due to the formation of metal atoms as a result of reduction of metal ions by complexes. (iii) The termination stage; it involves the determination of the last shape of the nanomaterials. This stage determines the size and shape of the nanomaterials such as nano prisms, nano hexahedrons, nano tubes, nano rods among others. The last phase is influenced mainly by the stabilizing capability of the plant extract. The higher the surface energy possessed by the nanomaterials, the less stability thus it is able to obtain a more stabilized morphology since it can easily change its shape *(*Akbar *et al*., 2020).

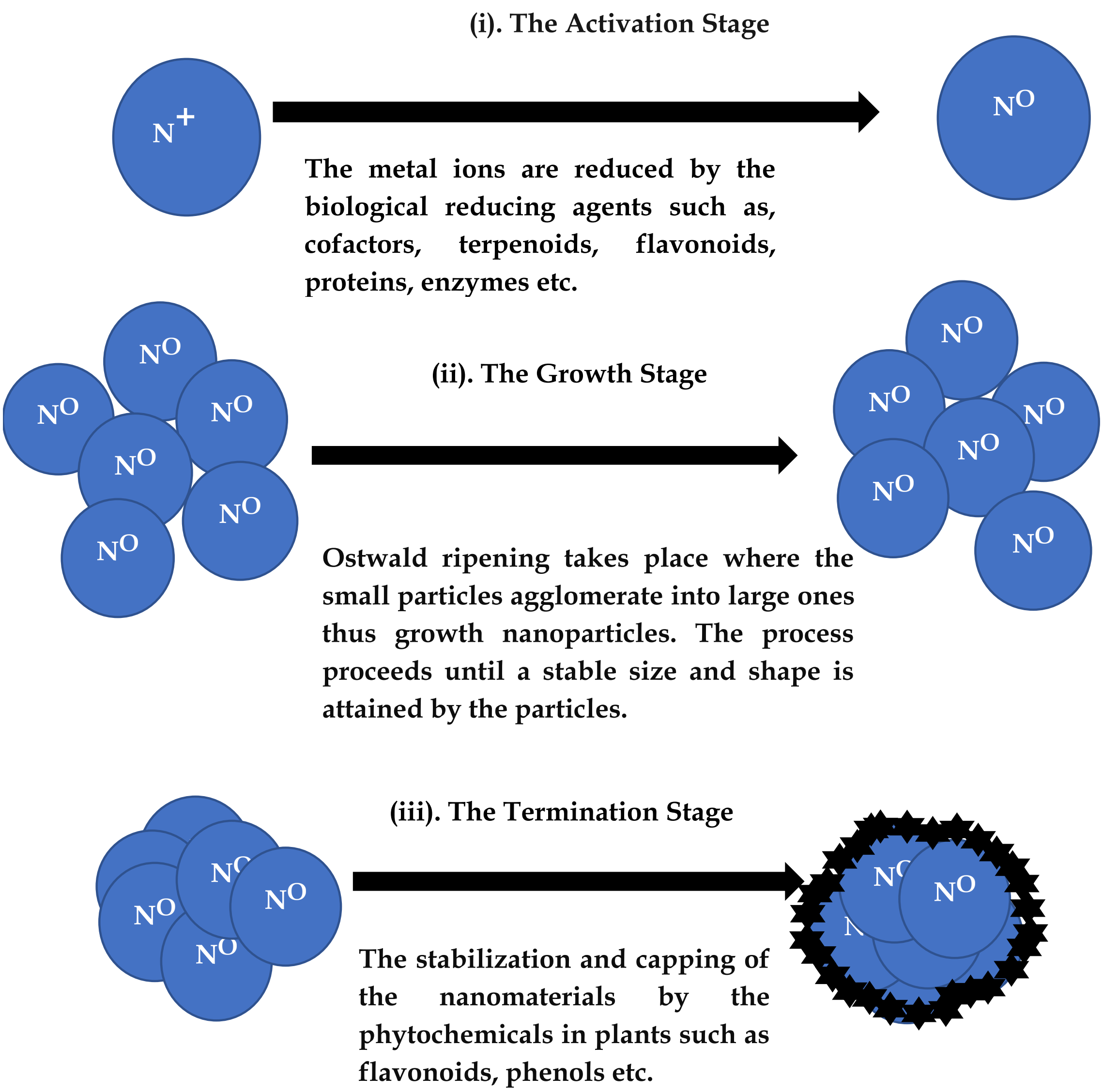

Figure 2.1: The proposed mechanism of green-synthesis stages of the metal oxide nanoparticles

Metal oxide nanoparticles eco-friendliness can be increased by having their surfaces coated with green biomolecules thus making them biocompatible. The commonly used hydrophilic polymers are protein, chitosan, polysaccharides, dextran and starch that improves the bioactivity of nanoparticles. The coupling of phytochemicals with nanomaterials during the nucleation phase strangely increases their dispersity and stability in aqueous solutions (Ahmed *et al*., 2021). In green chemistry, the secondary metabolites present in plants especially flavonoids have unique characteristics by acting as capping and reducing agents in the preparation of nanoparticles (P. Singh *et al*., 2020). These phytoconstituents play a vital part as antibacterial agents, reducing the precursor salts and metal ions intake *(*Garibo *et al*., 2020).

Nanomaterials are considered unstable while they are naked due to easier aggregation which leads to fading catalytic recycling and catalytic activities. This makes its industrial applications unattractive because of the disadvantage. The carbon and metal oxide nanoparticles are immobilized with polymers acting as agents of protection to avert the agglomeration of the nanoparticles (Veeramani *et al*., 2021).

Technology based on nanoparticles is vital in food, cosmetic, pharmaceutical and biomedical industry. The NPs are synthesized and applied in strengthening of materials, diagnosis, emulsions stability, delivery of target substances, refining agricultural yield and food excellence, nano fertilizers, nano pesticides and nano sensors due to the existence of bioactive materials (Plucinski *et al*., 2021). The ZnO nanoparticles have extraordinary optical properties, and admirable chemical as well as thermal stabilities. They are excellent semiconductors which is very significant (Pal *et al*., 2018). Zinc oxide nanoparticles are reported to have been applied in biological and pharmaceutical industries due to its unique characteristic to absorb the UV-Vis spectra in the range of 260 nm to near 400 nm (Ansari *et al*., 2020). The researchers have noticed the problems associated with the chemical synthesis of nanoparticles such as the tiresome use of long methods, long reaction times, great loss of energy, costly catalysis and the use of harmful and volatile solutions. The biogenic synthesis is studied therefore to improve output and reaction procedures (Ghamari Kargar *et al*., 2021). Table 2.1 shows some plants used in synthesis of copper oxide and zinc oxide nanoparticles.

Table 2.1: List of some plants and their secondary metabolites used in biosynthesis of copper oxide NPs and zinc oxide NPs

Plant and part extracts	NPs type and metal salt	Size and shape	Biomolecules	References
Ginger and garlic (Root extracts)	CuO NPs (Copper (II) nitrate)	23.38–46.64 nm; spherical	Amino acids, carbonyl group and aliphatic nitro compounds	(Ul-hamid *et al*., 2022)
Solanum torvum (L) (Leaf extracts)	ZnO NPs (Zinc nitrate)	28.24 nm; spherical	Polyphenols (quercetin), phenols, alkaloids, flavonoids and primary amines	(Maduabuchi *et al*., 2019)
Pomegranate (*Punica granatum*) (Leaves and flowers extracts)	ZnO NPs (Zinc nitrate hexahydrate)	57.75-52.50 nm; flower-like	Flavonoids, polyphenols and alcohols	(Ifeanyichukwu & Fayemi, 2020)
Aquilegia pubiflora (Leaf extracts)	ZnO NPs (Zinc acetate dihydrate)	34.23 nm; spherical or elliptical	Flavonoids and hydroxy-cinnamic acid derivatives	(Jan *et al*., 2021)
Parthenium hysterophorus (Leaf extracts)	ZnO NPs (Zinc nitrate)	16-45 nm; quasi-spherical, radial and cylindrical	Primary amines and nitriles	(Datta *et al*., 2017)
Eryngium caucasicum Trautv (Leaf extracts)	Cu NPs (Cupric nitrate trihydrate)	Less than 40 nm; Nearly spherical	Phenolic and flavonoids functional groups	(Journal *et al*., 2020)
Myristica fragrans (Fruit extracts)	ZnO NPs (Zinc acetate dihydrate)	41.23 nm; spherical or elliptical	Phenols and carbohydrates	(Faisal *et al*., 2021)
Ailanthus altissima (Fruit extracts)	ZnO NPs (Zinc nitrate hexahydrate)	5 -18 nm; Spherical	Flavonoids and phenolic compounds	(Awwad *et al*., 2020)
Aloe barbadensis. (Leaf extracts)	CuO NPs (Copper sulphate)	60-100 nm; spherical and cubic	Phenolic and alcoholic compounds	(Batool & Mehboob, 2018)
Bougainvillea (Flowers extracts)	CuO NPs (Copper acetate monohydrate)	12±4 nm; spherical	Primary amines of proteins and phenols	(Shammout & Awwad, 2021)

Sugarcane juice	CuO NPs (Copper nitrate)	22-30 nm; Square, rectangular, cubic cylindrical and spherical	Phenolics and polysaccharide fraction	(Mary *et al*., 2019)

2.2 The prevalence of Drug Resistant Pathogens in Medicine

Studies shown that the leading contributor of burden globally are bacterial illnesses. The bacterial species such as *Staphylococcus aureus*, *Staphylococcus intermedius, Staphylococcus hyicus, Acinetobacter pyogenes* and *Escherichia coli* developed resistance against antibiotics such as neomycin, sulfamethoxazole, amoxicillin-clavulanate, oxytetracycline, streptomycin, chloramphenicol, benzylpenicillin and ampicillin. There is an urgent need to invent new chemical methods that are safe, effective, cheap and new to synthesize antimicrobial drugs naturally from available resources due to the persistence of many drug resistant pathogens or bacterial strains thus posing is a need to curb antibacterial resistance. Many plant species contain phytochemicals-secondary metabolites that provide defense from plants. Plants, naturally, cannot move and are therefore prone to attacks resulting from human activities, bacteria, fungi, arthropods and herbivorous animals existing in the environment around them. The most interested parts of plants by researchers are stem barks, leaves and roots in search of bioactive molecules that intercept and interact with the agents which are unfavorably infective and might cause great harm to the plants. It is considered that biomolecules are mostly found in natural products (Infections, 2022).

The transmittable illnesses are posing a threat especially emerging hospital contagions due to the contaminations. The drug resistant pathogens like *Staphylococcus* are reported to be a vital encounter in the whole world. It has resisted several recent antibiotics. This issue requires invention or the use of recent antibacterial compounds or nano-biotics. Nanoparticles' efficacy against microbes can be increased by using metabolites of plants. The plant synthesized nanoparticles suppress the genes that are resistant by induction of antibiotic vulnerability (MRSA genes suppressed by the *M. officinalis* main components like Honokiol and Magnolol *(*Gilavand *et al*., 2021).

It was reported in a survey (of year 2000) by NINSS (Nosocomial Infections National Services) that about 30 % of people had been infected by microbial wound diseases in the whole world. Health-care expenses had risen by a great range almost every year. *Hemolytic streptococci, staphylococcus aureus* and *Pseudomonas aeruginosa* are bacterial strains that are aerobic as well as anaerobic that infect the wound surfaces (polymicrobial) thus known as pathogenic micro-organisms *(*Sethuram *et al*., 2021).

The magical agents or nanoparticles attack the microbe cells using several pathways making their escape hard. The Multi-Drug Resistance by microbes has caused a great problem globally since they resist drugs through development of resistant genes. The green synthesized nanoparticles (zinc and silver) revealed to be effective against *E. coli* in the inhibition zone of the range 21-22 ±3 mm. The best results were seen against MRSA(methicillin-resistant- *Staphylococcus-aureus*) in the range of 16-17 ±3 mm (Irfan *et al*., 2021).

The several identified drug resistant microbes (Multi Drug Resistant) in medicine included *Enterobacter, Pseudomonas, Acinetobacter, Klebsiella, Staphylococci, Enterococci* species etc. They are possessing a great challenge to humans. The microbes are showing great resistances towards Methicillin, Vancomycin, Carbapenems and Cephalosporins known to be worldwide leading antibiotics. They do so by showing effluence mechanism, reducing permeability of antibiotic drugs to their cell-walls, changing drug active sites and deactivating the enzymes. In addition, fungi such as Candida species are displaying resistances to different anti-fungal medicines like azole. These microorganisms are leading to severe diseases namely *tuberculosis, diarrhea,* severe *bacteremia, cholecystitis, meningitis, osteomyelitis, sepsis, pneumocystis pneumonia, candidiasis* and *aspergillosis* that threaten life (Khan *et al*., 2020).

In comparison with inorganic anti-microbial agents, research has confirmed that organic substances are not fit at extremely high temperatures. The microbes possess a negative charge while the nanomaterials a positive charge. An electromagnetic attraction is developed between the target bacteria and the metal nanoparticles during interaction. This is as a result of strongly reactive single oxygen in the metal oxide nanomaterials (Sedlmeier *et al*., 2020). The extracts from microorganisms and florae are used to reduce and stabilize the nanomaterials synthesized. Usually, the antioxidants acquired naturally from plants are involved in reduction of metal ions such as gold and silver positive ions. Many studies have been developed for the assessment of antioxidant properties of several phyto-constituents *(*Cardoso-Avila *et al*., 2021*)*.

The ZnO nanomaterials possess the antimicrobial behavior by interacting electrostatically with bacterial cell surfaces. This cytotoxic property is as a result of creating pores on bacterial cell surfaces thus causing leakage of the contents in cytoplasm and finally killing the cell. This inhibits bacterial growths. The carbonyl groups on the microbial cells surfaces causes them to be negatively charged and ZnO nanomaterials in aqueous solutions possess positive charges (Akbar *et al*., 2020*)*.

The release of positive silver ions can be in several forms like polymeric degradation or diffusion in polymer matrix swelling. The monitored release of drugs is vital for long-lasting antimicrobial activities. The metal oxide nanoparticles are fabricated to improve biodegradability and behave like nanofibers. The nanoparticles are applied and kill bacteria by preventing replication and cell respirations in eukaryotic as well as prokaryotic cells. The behavior of nanoparticles is affected by fiber morphology, size and shape (Sethuram *et al*., 2021). Nanoparticles are also called wonder-of-modern medicine. Nanoparticles are estimated to destroy 650 bacterial cells while antibiotics destroy only half-dozen of microbes (Akbar *et al*., 2020*)*.

Nanoparticles have been introduced in clinical medicine to cure leishmaniasis. This is the current application since patients declined the use of pentostam and glucantime due to their adverse effects in treatment. It was for over 60 years known as up-to standard treatment. These agents have several toxicities and are no longer used because of long treatment periods, pain during administration and increased parasite resistance (Gharby, 2021).

2.3 Various applications of nanotechnology

The current art of expertise confirmed to be well-thought-out is nanotechnology. The abundant entrenched divisions in engineering fields included pharmacological, chemical, nutrition processing production and power-driven. It has also played a motivating part in areas of environmental sciences, power generation, optics, computation and drug delivery. This strategy on its arrival has established numerous nanoscale strategies by several means like chemical, green approaches and physical means*(*Faisal *et al*., 2021). The antibacterial applications of bioinspired synthesized inorganic nanoparticles have been appreciated mostly in various ways such as;

Treatment of physical wounds, (2) Microorganism pathogens in humans and (3) pathogens inhibition in foods. This is why these NPs can be used for medical purposes *(*Kobylinska *et al*., 2020*).* Chemical solution synthesis in the fabrication of nanoparticles isn't safe compared to biogenic green synthesis using plant extracts *(*Perveen *et al*., 2020*).*

Green route synthesis by consideration of several plant parts yielded materials that are active and have superior potential against gram negative as well as gram positive microbes and diverse tumor cells. They displayed advanced properties that are antioxidant than those of thermal, physical and chemical methodologies. Therefore, plant natural compounds and bio-units of microorganisms are given higher urgency in rigorous explorations amid dissimilar bio-tools to synthesize nanoparticles (Devanesan & AlSalhi, 2021).

The nanoparticles are small in size (nano-sized) which makes them qualify to easily pass through the cellular membranes. This is also due to homogeneity caused by their small sizes and can distribute uniformly in the cells upon application in medicine in drug delivery against microbes, cancer therapy and bacteria. In addition they can also be used in cryogenic material superconductivity, agricultural and catalytic processes *(*Kobylinska *et al*., 2020*).* In nanoscience, nanoparticles are mostly in the size of 1-100 nm. The metal oxide nanoparticles synthesized in the nm area are effective in bacterial as well as fungal treatment because microorganisms are between 100-micrometers in size (Bayat *et al*., 2019).

Nanomaterials have considerably gained attraction in fields like nanomedicine, material strategy, food and cosmetic industry. Nanoparticles have advantageous properties to be applied in medicine to treat and detect several kinds of gastrointestinal illnesses, neurodegenerative, arthritis, inflammation, fibrosis and cancer. They are also used as nanodevices in medicine, biosensors and drug delivery options (Sousa De Almeida *et al*., 2021).

The metal oxide nanoparticles with varying structures and morphologies are synthesized using various procedures for effectual and fast detections of hydrogen gas. The responses have been greatly increased with evolution of nano-technology. Nevertheless, the practical application of hydrogen sensors has been hampered by feeble durability, poor steadiness and low selectivity. Therefore, the studies of metal oxide nanoparticles for hydrogen sensors had been done (Shi *et al*., 2021). (Han *et al*., 2021) reported that, ‘’Nanomaterials have been suggested as promising eco-friendly and harmless insecticides. There are many nanoparticles used as insecticides and nematicides against *Meloidogyne incognita*, which is a biotrophic parasite of crops. It is important to research the dependence of the physiological activity of *B. xylophilus* on nanomaterials.’’

It was discussed by *(*Taherzadeh Soureshjani *et al*., 2021*)* that the P-type semi-conductors are applied in antibacterial activities, pigments, solar cells, photocatalysis and catalysis like copper oxide nanoparticles. The nanoparticles are used to kill the bacteria by producing ROS (Reactive oxygen species) and releasing copper ions.

However, nanoscale materials have tried to solve many biological sciences related problems or issues such as environmental, chemical and physical. The nanomaterials are applied in agriculture amongst many fields as an antibacterial agent by monitoring wastes (pesticides’ by-products) and a stress condition in plants. These wastes result from wrong practices applied in agriculture (P. Singh *et al*., 2021). Nano-fertilizers have been invented to improve the yields in agriculture. It is substance that takes or carries various crop nutrients using different forms; 1) emulsions or particles taken in the nanometer range, 2) with coatings of thin-polymer films and 3) captured in the nanoparticles (nano-porous network). The most researched inorganic oxides are zinc, copper and iron since they are more promising and much studied (Leonardi *et al*., 2021*)*.

The nanoparticles have been improved or developed for therapeutic and imaging in clinical study. The specific and sensitive functional and anatomical properties are as a result of the nanoparticles (Imaging Agents) in different clinical techniques for imaging (Contrast Imaging Techniques). The nanoscale particles possess a capability to respond to specific micro-environmental conditions, biological testing and external stimulus thus branded "smart-nanomaterials" (Pellico *et al*., 2021).

2.4 *Entada abyssinica* species in medicine

It was concluded that the methanol stem bark extracts of *Entada abyssinica* are not toxic on histological, haematological and biochemical indices. The secondary metabolites were reported to be antimicrobial, antioxidant and cytotoxic. Mass spectroscopy and NMR spectra were used to characterize the *Entada abyssinica* isolated components from the stem barks which included 1′,2,6′-bis-[(S)- 2,3-dihydroxypropyl] hexacosanedioate, monoglyceride, entadanin and peltogynoid. The phytochemical screening of methanol extracts of *E.africana* and *E.abyssinica* possessed coumarins, glycosides, steroid, flavonoids, triterpenes, tannins and alkaloids as metabolites in dominance (Obakiro, Kiprop, Kigondu, K'owino, *et al*., 2021).

2.5 *Warburgia ugandensis* species in medicine

Warburgia ugandensis (WU) has several names such as Ugandan greenheart, pepper bark tree and East African greenheart. Its extracts constitute of sesquiterpenoids, drimane, terpenoids and many other secondary metabolites which are antimicrobial. These metabolites possess therapeutic activities against measles, weak joints, constipation, urinary tract infections, muscle pain, oral thrush, fever, stomachache, bronchial infections, common cold, snake bites, toothache, sexually transmitted diseases, cough, diarrhea and malaria (Okello & Kang, 2021).

Warburgia ugandensis belongs to Canellaceae family mostly found at drier Kenyan, Ugandan and Ethiopian high-lands and rain-forests (Gonfa *et al*., 2020). *Warburgia ugandensis* extracts were used to cure HIV virus in Eastern Africa as a well-known medicinal-plant (Anywar *et al*., 2021). Kraus *et al.* (Kraus *et al*., 2021) reports that the high efficacy of *Warburgia ugandensis* in the treatment of ailments is due to the presence of phytoconstituents belonging to mannitol, tannins and drimane sesquiterpenes groups. The three shown anti-fungal activity against *Sclerotinia libertiana, C. utilis, Candida albicans* and *Saccharomyces cerevisiae.*

2.6 Analysis Techniques

2.6.1 Gas Chromatography – Mass Spectrometry

This is considered as one of the most effective analysis method used to detect and characterize (structure of phytochemicals) of various bioactive compounds present in the extracts of plants (Cupido *et al*., 2022). Usually, the phytoconstituents are mostly extracted using steam distillation, maceration and solvent techniques. The application of UAE (ultrasound-assisted extraction) methodology has not yet been well reported (Asmira Abd Rahim *et al*., 2018). The identification of phytoconstituents in plant extracts as confirmed in GC-MS profiling, dictates their importance in medicine as therapeutic agents (Olivia *et al*., 2021). Table 2.2 shows various chemical compounds obtained in GC-MS technique and their activities in medicine.

Table 2.2: The summary of the phytochemical activities of some of the compounds present in *Warburgia ugandensis* and *Entada abyssinica* from literature

S.NO	Name of the compound	Class	The phytochemical activity	References
1	D-Limonene	Menthane monoterpenoids	Antioxidant, antituberculosis, anticancer, analgesic, anticonvulsant, anti-inflammatory antimicrobial and antiviral biological potentials.	(Zielińska-Błajet & Feder-Kubis, 2020)
2	Triacetin	triacylglycerols	Anti-inflammatory and antioxidant properties.	(Zhang *et al*., 2019)
3	Diethyl Phthalate	phthalate	Insecticidal, antimicrobial and allelopathic activities.	(Huang et al., 2021)
4	Hexadecanoic acid, methyl ester	Fatty acid methyl esters	Possess anti-inflammatory, antimicrobial and antioxidant activities.	(Siswadi & Saragih, 2021)
5	Corymbolone	Essential oil	Anti-inflammatory, anaesthetic, antispasmodic, antiseptic, antipruritic, anthelmintic, analgesic and several other disease control and therapeutic uses.	(Umaru *et al*., 2019)
6	Isoshyobunone	sesquiterpenoids	Antiviral, insecticidal,	(Jiang *et al*., 2021)

			antitumor, anti-inflammatory and anti-bacterial activities.	
7	Phytol	Diterpene alcohol	Anti-inflammatory anti-HIV, antifertility, neurotrophic, cholesterol-lowering and anticancer effects.	(Nie *et al*., 2021)

2.6.2 UV-Visible (UV-Vis) Spectroscopy

The aqueous concentrations of the samples were optically studied to obtained results by using the UV-Vis spectroscopy technique. A graph of wavelength versus absorbance was plotted for demonstration in order to locate maximum surface plasmon resonance peaks (Ikhioya *et al*., 2023).

2.6.3 Fourier-transform infrared spectroscopy

The FTIR technique was used to identify the functional groups (bonds in biomolecules) and various chemical compounds (phytochemical constituents) involved in the reduction, capping and stabilization of the synthesized nanoparticles (Bhavyasree & Xavier, 2020). The FTIR spectra were obtained in the range 4000-400 cm^{-1}.

2.6.4 X-Ray powder Diffraction (XRD)

To patterns obtained in XRD technique (in 2θ range 10-140°) are used in the identification of the structural crystallinity of the synthesized nanoparticles (Selim *et al*., 2020). The patterns are also applied in Scherrer's equation to calculate the particles sizes.

CHAPTER THREE

METHODOLOGY

3.1 Instruments and apparatus

Gas Chromatography-Mass Spectrometry (GC-MS Qp2010SE model), UV vis spectrophotometer (UV 1800, Schimadzu model), Fourier Transform Infrared Spectrophotometer (IRAffinity-1S, SHIMADZU model), XRD (D8 Advance X-ray Diffractometer system model), Oven, Centrifuge, Hot plate, Magnetic stirrer, Filter papers (Whatman No. 1), Analytical balance (digital electronic) and Petri dishes were used in this study.

3.2 Chemicals and reagents

Sodium hydroxide, Iodine solution, Alkaline reagent, Molisch's reagent, Ferric chloride, Lead acetate, Wagner's and Mayer's reagent, tannic acid, aluminium chloride, sodium nitrite, Gallic Acid, picric acid, sodium carbonate, Folin-Ciocalteu reagent, distilled water, DPPH solution and Methanol. Bacterial strains (*Escherichia coli* and *Staphylococcus aureus*), *Entada abyssinica* leaves and *Warburgia ugandensis* leaves. Zinc-acetate Di-hydrate precursor, Cupric nitrate (Tri-hydrate) precursor and distilled water. The chemicals were purchased at Reno Chemicals and Lab Equipment Suppliers, Eldoret while the Nutrient Agar was purchased at Commercial Enterprises, KEMRI, Kenya.

3.3 Sample collection

The leaves of *Entada abyssinica (Figure 3.1)* and *Warburgia ugandensis (Figure 3.2)* were collected from Kenya Plant Health Inspectorate Services (KEPHIS), Kitale Branch, in Tranzoia County, Kenya. They were identified by Dr. BK Wanjohi (taxonomist) from the Forestry Department, University of Eldoret.

Figure 3.1: ***Entada abyssinica*** **fresh leaves (Photo by Author, 2020)**

Figure 3.2: ***Warburgia ugandensis*** **fresh leaves (Photo by Author, 2020)**

3.4 Preparation of plant extracts

The freshly acquired leaves were washed thoroughly with tap and distilled water to eliminate the particles of dust and air-dried at room temperature. The dried leaves were grinded to powder form. The extract solutions of the plants were obtained by boiling 10 g of the grounded leaves in 200 mL of distilled water for 1 hour maintained at temperatures between 70-80 °C. The mixture was stirred rapidly by means of a magnetic stirrer. The extracts were then refrigerated at 4 °C after filtration by a filter paper (Whatman No. 1) awaiting further experimental procedures (Demissie *et al*., 2020).

3.5 Phytochemical screening

Qualitative analysis

The phytochemical screening was carried out to determine the presence of alkaloids, saponins, phenolic compounds and flavonoids that are responsible for the reduction, encapsulation and stabilization of the nanoparticles.

3.5.1 Saponins test

Frothing test was carried out to detect the presence of saponins as reported by (Muhongo *et al*., 2021). About 20 mL of distilled water was used to dilute 60 mg of the plant extract. The suspension obtained was for 20 min vigorously shaken and incubated for 25 min. The presence of saponins was indicated by a foam layer above the surface.

3.5.2 Flavonoids test

Alkaline reagent test was performed to detect the presence of flavonoids as reported by (Ezeonu & Ejikeme, 2016). 10 % solution of ammonium hydroxide was used to treat an extract solution in aqueous form. The presence of flavonoids was indicated by a yellow fluorescence.

3.5.3 Phenolic Compounds test

The Lead acetate test was performed to detect the presence of phenolic compounds. 4mL solution of 10 % lead acetate was added to 60 mg of aqueous plant extract. The existence of a white precipitate that was bulky indicated the phenolic compounds presence (Shaikh *et al*., 2020).

3.5.4 Alkaloids tests

Hager's test method was used to detect the presence of alkaloids. A few drops of dilute HCl were used to dilute 60 mg of extract that was free of the solvent and filtered. The filtrate in few mL was added 3 mL of picric acid that was in saturated aqueous form (Hager's reagent). The presence of alkaloids was indicated by the existence of a prominent orange precipitate (Shaikh *et al*., 2020).

3.6 Qualitative analysis using GC-MS technique

The methanolic crude plant extracts of *Entada abyssinica* and *Warburgia ugandensis* leaves were subjected to GC-MS analysis. The sample clean-up was carried out to remove the matrices that could cause the interference. The analyte was concentrated to change the sample matrix.

The C18 cartilage was conditioned with 3 mL of methanol then 3 mL of sample was loaded. It was allowed to flow slowly out of the cartilage giving it adequate time to interact with adsorbent. Then it was left to dry in a stream of air for twelve minutes. It was thereafter eluted with 3 mL of methanol into a 4 mL vial. It was then concentrated using a genetic concentrator, reconstituted with 1 mL of methanol, filtered using nylon micro filters size of 0.22 µm into 1.5 mL vials and taken to GC-MS for analysis.

The column oven temperature was 55 °C and ion source temperature was 200 °C. The flow rate of helium as carrier gas was 1.2 mL/min. The capillary column of dimensions 30 meters × 0.25 mm (id) was used. The injection mode was split. Electron ionization mode was at 70 eV while the range of mass was at 40 – 400 m/z.

3.7 Quantitative analysis

3.7.1 Total Phenolic Content determination

The procedure used was adopted from (Soni *et al*., 2018). The serial dilutions of working standards of concentrations 1.25, 2.5, 3.75, 5.0 and 6.25 µg/mL in labelled test tubes T_1, T_2, T_3, T_4 and T_5 respectively were prepared from pipetted aliquots of 0.1, 0.2, 0.3, 0.4 and 0.5 mL respectively. 25 µL of sample extracts of phenolics were prepared in test tube series and analysis carried out in triplicates. Distilled water was used to top up the test tube contents to 1 mL. Distilled water was also used as a blank in 1 mL volume. To all the test tubes including that of the blank, 1 mL of 0.5 N Folin-Ciocalteu was added. The vortex was used to mix the test tubes' contents and at room temperature allowed to stand for 8 min. Including the blank, all the test tubes were added 5 mL of 10 % sodium carbonate and vortex. At room temperature, the test tubes were for 40 min incubated in the dark. The spectrophotometer at 725 nm was used to measure the blue color absorbance that was obtained against the blank reagent.

$$C = c_1 \, x \, \frac{V}{m} \tag{1}$$

Where C = total phenolic content in mg/g, in GAE (gallic acid equivalent), c_1 = concentration of the Gallic Acid established from the calibration curve in mg/mL, V = volume of extract in mL and m = the weight of the plant extract in g. The equation 1 above was applied to calculate the amount of phenolics in the sample quantitatively, that is, mg/g of the Gallic Acid Equivalent.

3.7.2 Total tannin content determination

The determination of the total content of tannins was adopted from (Selvakumar *et al*., 2019) with few modifications. 2 mL Eppendorf tubes, 50 mg of polypyrrolidone (PVPP) was weighed. Two hundred and fifty µL of distilled water and 250 µL of the sample of plant extract was added. The Eppendorf tubes were incubated at 4 ºC for 4 hours and later centrifugated for 10 min at 3000 rpm. The non-tannin phenolic was only contained in the supernatant. The serial dilutions of working standards of concentrations 1.25, 2.5, 3.75, 5.0 and 6.25 µg/mL in labelled test tubes $T_{1,}$ $T_{2,}$ $T_{3,}$ T_4 and $T_{5,}$ respectively were prepared from pipetted aliquots of 0.1, 0.2, 0.3, 0.4 and 0.5 mL respectively. To a series of test tubes, 50 µL of the supernatant containing the non-tannic phenolic content was added and the analysis was carried out in triplicates. Distilled water was used to top up the test tube contents to 1 mL. Distilled water was also used as a blank in 1 mL volume. To all the test tubes including that of the blank, 1 mL of 0.5 N Folin-Ciocalteu was added. The vortex was used to mix the test tubes' contents and at room temperature allowed to stand for 8 minutes. Including the blank, all the test tubes were added 5 ml of 10 % sodium carbonate and vortex. At room temperature, the test tubes were incubated in the dark for 40 minutes. The spectrophotometer at 725 nm was used to measure the blue color absorbance that was obtained against the blank reagent.

$$C = c_1 \, x \, \frac{V}{m} \tag{2}$$

Where C = total tannin content in mg/g, in TAE (Tannic acid equivalent), c_1 = concentration of the Tannic acid established from the calibration curve in mg/ml, V = volume of extract in mL and m = the weight of the plant extract in g. The equation 2 above was applied to calculate the amount of tannins in the sample quantitatively, that is, mg/g of the Tannic Acid Equivalent.

3.7.3 Total flavonoid content determination

The analysis was carried out as reported by (Roy M *et al*., 2018) with few modifications. The serial dilutions of working standards of concentrations 4, 8, 12, 16 and 20 µg/mL in labelled test tubes T_1, T_2, T_3, T_4 and T_5, respectively were prepared from pipetted aliquots of 0.1, 0.2, 0.3, 0.4 and 0.5 mL respectively. 25 µL of sample extracts of flavonoids were prepared in test tube series and analysis carried out in triplicates. Distilled water was used to top up the test tube contents to 1 mL. Distilled water was also used as a blank in 1 mL volume. To all the test tubes including that of the blank, 75 µL of 10 % sodium nitrite was added. The tubes were mixed using a vortex and allowed to stand for 8 minutes at room temperatures. All test tubes were added 300 µL of 5 % aluminum chloride, mixed using a vortex and allowed to stand for 6 minutes at room temperatures. Two mL of 4 % NaOH was added to all test tubes and the volume topped up to 5 mL using distilled water. The contents were vortex and left to stand for 10 minutes at room temperatures. The spectrophotometer at 510 nm was used to measure the pink color absorbance that was obtained against the blank reagent.

$$C = c_1 x \frac{V}{m} \tag{3}$$

Where C is total flavonoid content in mg/g, in RAE (Rutin acid equivalent), c_1 is the concentration of the Rutin acid established from the calibration curve in mg/mL and V is the volume of extract and m = the weight of the plant extract in g. The equation 3 above was applied to calculate the total flavonoids in the sample quantitatively, that is, mg/g of the Rutin Acid Equivalent.

3.7.4 Total alkaloid content determination

The procedure for the determination was adopted from (Khanal, 2021). Ninety mL of 10 % acetic acid was used to dissolve 5 grams of dried sample. After shaking, it was allowed to stand for 3.5 hours and later filtered using Whatman No. 1 filter paper. The hot plate was used to evaporate filtrate while stirring to a quarter of the original capacity. The alkaloid contents were precipitated using NH_4OH (Concentrated Ammonium hydroxide) dropwise. 1% NH_4OH was used to wash the solution that was filtered again. The precipitate present on the filter paper was dried in the oven for 25 minutes at 60 ^{0}c. It was allowed to cool and weighed.

$$Alkaloid\% = \frac{W2-W1}{W2} \times 100 \tag{4}$$

Where, W1= empty filter paper's weight

W2= alkaloid precipitate + Weight of paper

3.7.5 Total saponin content determination

The procedure followed was adopted from (Khanal, 2021). Ninety mL of 50 % alcohol was mixed with 25 mL of plant extract and boiled for 35 minutes in a round bottomed flask. It was then filtered while still hot. Three grams of charcoal was then added to the filtrate. It was filtered after boiling. Acetone was used to precipitate the saponins after adding to the cooled filtrate. The precipitate of saponins was collected.

$$The\ \%\ saponins$$

$$= \frac{W2 - W1}{W2} \times 100 \tag{5}$$

Where, W_2= The weight of residue

W_1=Weight of filter paper

3.8 Biosynthesis of ZnO Nanoparticles

The ZnO nano-structures were synthesized following a procedure developed by (Kahsay *et al*., 2019) with few important modifications. Seventy mL of 100 mM Zinc Acetate Dihydrate solution was added to 15 mL of plant extract while constantly stirring using a magnetic stirrer. The four separate mixtures were run for 20, 30, 40 and 60 minutes, respectively. The reaction mixture was heated under continuous stirring at temperatures of 50 °C -60 °C. The change in color to yellowish indicated the synthesis of zinc oxide nanoparticles. The product was centrifuged and washed in two cycles with distilled water for the removal of precursors that had unreacted. Zinc oxide nanoparticles formed were dried overnight at 30 °C in an oven. The procedure was repeated at varied pH of 9, 10 and 11.

3.9 Biosynthesis of C*u*O Nanoparticles

The biosynthesis of copper oxide nanoparticles was carried out as by (Chowdhury *et al*., 2020) with some modifications. The hydrolysis procedure involved the application of a precursor (cupric nitrate (tri-hydrate) with the existence of extracts of leaves of *Entada abyssinica* and *Warburgia ugandensis* plant. Under continuous stirring at 60 °C, 20 mL of plant extract was added to 80 mL of 0.01 M $Cu\ (NO_3)_2$. $3H_2O$ solution in a conical flask. The four separate mixtures were run for 20, 30, 40 and 60 minutes, respectively. The reaction mixture was heated while continuously stirring at maintained temperatures of 50 °C -60 °C. The final reacted mixture was cooled down at room temperatures. The isolated product was then centrifuged for 15 minutes at 1000 rpm. The product isolated was purified by washing using distilled water and centrifugation. The washing was repeated twice (two cycles). The final product was dried in an oven overnight. The procedure was repeated at varied pH of 6.5, 8.5 and 10.5.

3.10Characterizations and analysis of the biosynthesized nanoparticles

3.10.1 UV-Visible (UV-Vis) Spectroscopy analysis

To obtain the optical characteristics of the green route synthesized CuO and ZnO nanoparticles, each sample was subjected to UV-Visible spectrometry at a wavelength scan range between 190 nm to 1100 nm with a resolution of 4 nm. The nanoparticles were dissolved in distilled water and put in a UV VIS quartz cuvette. The surface-Plasmon resonance absorptions at specific wavelengths of the nanoparticles were recorded. DW (distilled water) was used as a blank.

3.10.2 Fourier-transform infrared spectroscopy (FTIR) analysis

The small quantities of the dried samples of nanoparticles were placed on a flat steel plate and compressed. The sample (on a sample holder) was run at a wavenumber of 400 to 4000 cm^{-1}. Fourier-transform infrared spectroscopy (IRAffinity-1S, SHIMADZU model) identified the functional groups involved in the stabilization and reduction of the nanoparticles.

3.10.3 X-Ray powder Diffraction (XRD) Spectral Analysis

The sizes (diameter) of the nanoparticles were obtained using X-Ray powder Diffraction. D8 Advance X-ray Diffractometer system model with Cu-Kα radiation; 40 kV, 40mA, λ =0.154 nm and 2θ values range of 10°–90° at 0.0194° increment was used to examine each sample (CuO NPs and ZnO NPs).

3.11 Anti-bacterial Evaluation Methods.

3.11.1 Agar-Disc Diffusion Method

Agar-disc Diffusion technique was used to evaluate the microbial potentials of the green-synthesized copper oxide and zinc oxide nanoparticles against *Escherichia coli* (Gram-negative) and *Staphylococcus aureus* (Gram-positive) nominated bacteria (Murthy *et al*., 2020), (Sharma *et al*., 2018). The bacterial strains were obtained from Kenya Medical Research Institute Laboratory. Twenty-eight grams of the nutrient agar was weighed and dissolved in 1 liter of distilled water in a conical flask. The solution was boiled gradually with constant stirring on a hot plate. The dissolved solution was capped with aluminum foil and autoclaved at 121 °C for 15 minutes. After sterilization, the pressure of the autoclave was allowed to return to zero before opening. The media was removed and left to cool to around 45 °C in a clean bench. The cap was removed carefully and the mouth of the flask flamed and then the media was dispersed in sterile petri dishes. After the agar has solidified, the bacteria cultures 0.1 mL were inoculated and spread using a sterile spreader. Filter paper discs (Whatman (NO.1), 3 mm radius) were punched and soaked with concentrations (250 ppm) of extracts, ampicillin and the synthesized copper oxide and zinc oxide nanoparticles and placed or positioned to the surface of the inoculated plates. The positive control that was considered was ampicillin discs. Then the ready set ups were incubated at 37 °C for twenty-four hours. The zones of inhibition were measured (in mm using a ruler) and quantified. The results were presented as mean± standard deviation of the triplicate values.

3.11.2 Statistical analysis-One-way ANOVA.

The anti-bacterial tests were conducted in triplicates. The SD (standard deviation) and average was calculated. The Excel spreadsheet software was applied to find the significance of the results ($p \leq 0.05$).

CHAPTER FOUR

RESULTS AND DISCUSSION

4.1 Phytochemical screening

Qualitative analysis

Different types of phytochemicals such as phenols, saponins, alkaloids and flavonoids as shown in (*Table 4.1)* were screened. Their presence supports the reason why these plants have been used to treat various ailments traditionally (Friday *et al*., 2020). It also supports their application in the synthesis of CuO and ZnO nanoparticles in this study.

Table 4.1: The qualitative phytochemical screening to determine the presence of the following phytochemicals in the leaf extracts of *Entada abyssinica* and *Warburgia ugandensis*

	Observation	
Test	EA	WU
Phenols	+	+
Saponins	+	+
Alkaloids	+	+
Flavonoids	+	+

Key

+= presence of components

-= absence of components

4.2 Quantitative analysis of total tannins, flavonoids, alkaloids, saponins and phenolic contents.

The analysis was carried out where total alkaloids and saponins content was obtained gravimetrically while total phenolics, tannins and flavonoids content were done by spectrophotometric technique at selected wavelengths (*Figures* 4.1, 4.2 and 4.3).

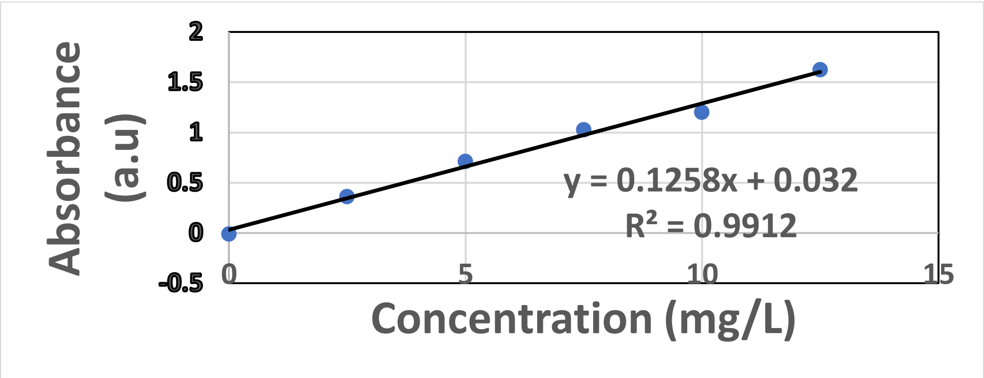

Figure 4.1: The standard calibration plot of total tannins content determination

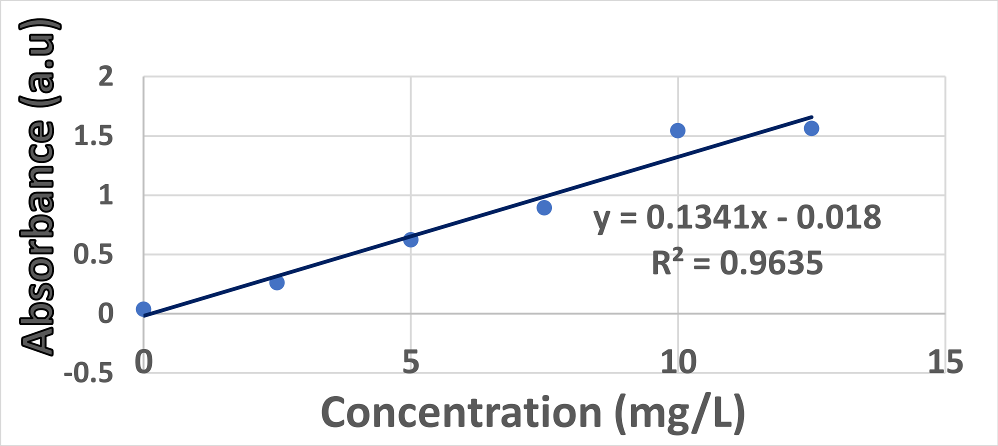

Figure 4.2: The standard calibration plot of total phenolics content determination

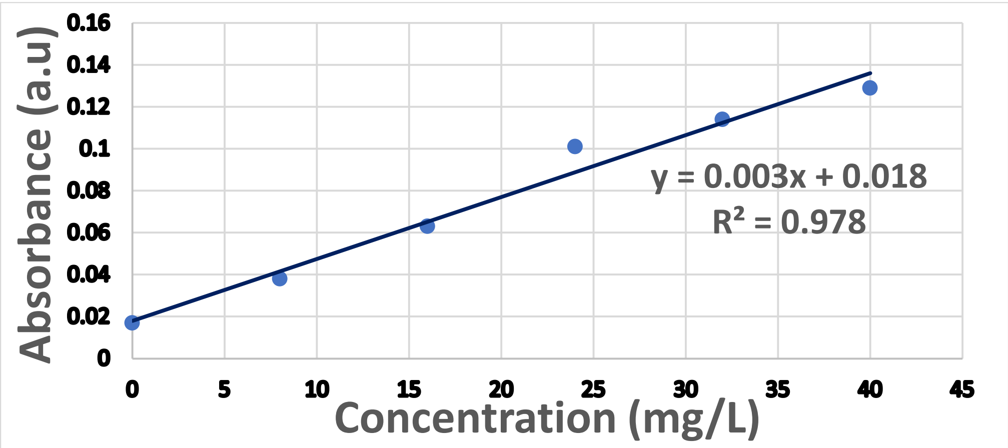

Figure 4.3: The standard calibration plot of total flavonoids content determination

The graphs in Figure 4.1, 4.2 and 4.3 shows the calibration curves drawn to determine the concentrations of tannins, phenolics and flavonoids using standards of tannic, gallic and rutin acids respectively. The R^2 values from the standard curves were 0.9912, 0.9635 and 0.978 respectively. The equations 1, 2, 3, 4 and 5 were used to calculate the total contents present in the dry samples. The results for total phenolics, flavonoids, saponins, alkaloids and tannins contents are shown in Table 4.2.

Table 4.2: The total phenolic, flavonoid, saponin, alkaloid and tannin contents of leaf extracts of *Entada abyssinica* and *Warburgia ugandensis*

Plant extracts	Total phenolic content (mg/g in GAE)	Total flavonoids content (mg/g in RAE)	Total saponins content (%)	Total alkaloids content (%)	Total tannins content (mg/g in TAE)
E.A extract	57.43±0.89	1375.39±24.23	0.94±0	1.27±0	4.77±0.13
W.U extract	19.45±0.42	959.84±17.50	1.33±0	1.42±0	0.66±0.13

The quantitative analysis of biomolecules in plants are concerned in anti-microbial and anti-viral activities (Selvakumar *et al*., 2019). Table 4.2 shows the results of total tannins, flavonoids, phenolic, alkaloids and saponins contents in the two plant varieties of *Entada abyssinica* and *Warburgia ugandensis* leaf extracts. The results acquired were expressed as mean ± standard deviation (SD) of the triplicate values. From the results obtained, *Entada abyssinica* had more phenolic, tannins and flavonoids contents compared to *Warburgia ugandensis.* The alkaloids contents in *Warburgia ugandensis* leaf extracts were more compared to *Entada abyssinica*. This briefly gives a supportive explanation on the medicinal activities of these plant leaf extracts in the treatment of various illnesses and formulation of nanoparticles.

4.3 GC-MS analysis of Entada abyssinica and Warburgia ugandensis extracts.

The GC-MS analysis revealed the presence and identity of various chemical compounds in the two species of plants as shown in (*Figure 4.4, 4.5, 4.6* and *4.7)* and (*Table 4.3* & *4.4)* when matched with NIST (National Institute of Standard and Technology) library.

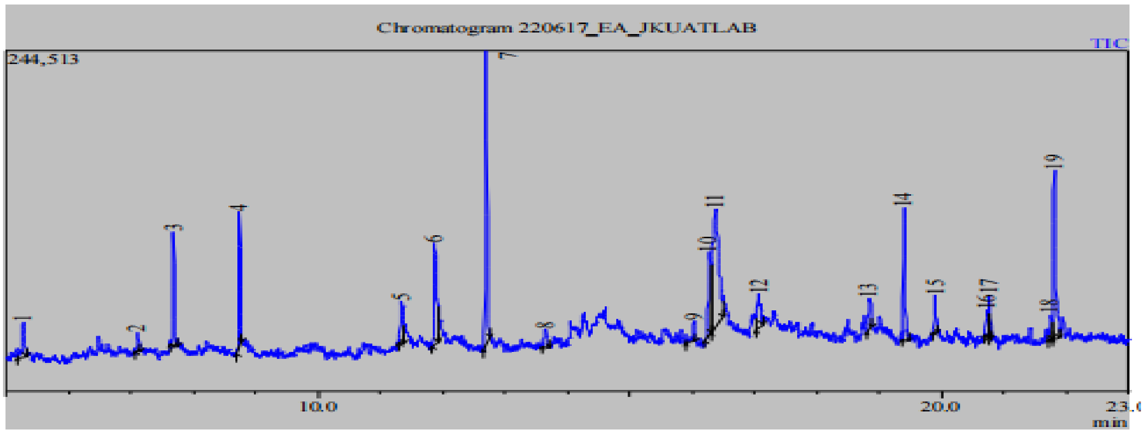

Figure 4.4: The GC-MS chromatogram of *Entada abyssinica* showing various chemical compounds compositions

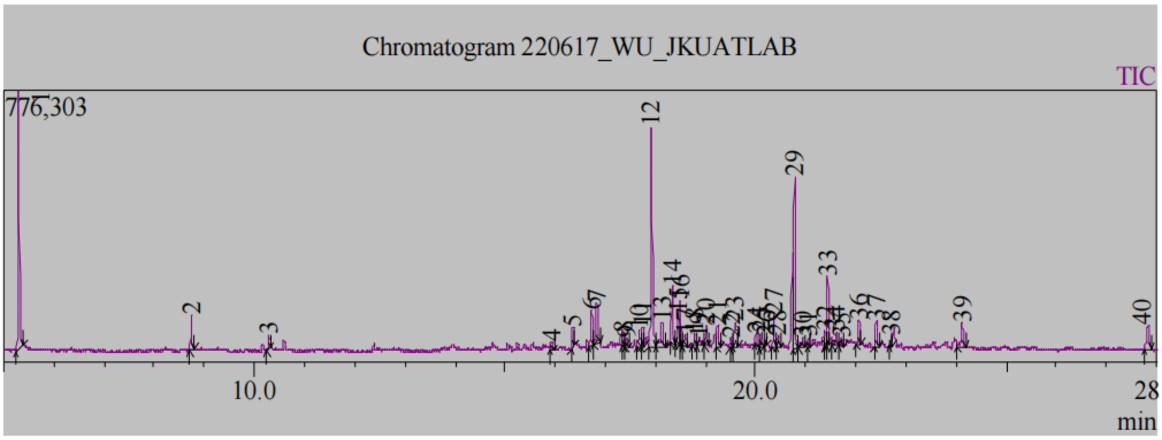

Figure 4.5: The GC-MS chromatogram of *Warburgia ugandensis* showing various chemical compounds compositions

Table 4.3:The list of some secondary metabolites of *Entada abyssinica* leaf extracts obtained from GC-MS technique with the reference of NIST 17 spectra information database

S.NO	RT	Name of the compound	M.W	Molecular Formula	% Peak area	Class
1	5.27	o-Xylene	106.16	C_8H_{10}	2.69	Xylenes
2	7.11	Benzene, 1,2,4-trimethyl-	78.11	C_9H_{12}	1.06	Hydrocarbon
3	7.68	D-Limonene	136.24	$C_{10}H_{16}$	5.58	Menthane monoterpenoids
4	8.74	Undecane	156.31	$C_{11}H_{24}$	6.17	Alkanes
5	11.34	2-Pentanol, TMS derivative	88.15	$C_5H_{12}O$	3.71	Alcohol
6	11.88	Caprolactam	7.27	$C_6H_{11}NO$	7.27	Caprolactams
7	12.70	Triacetin	218.21	$C_9H_{14}O_6$	13.87	Triacylglycerols
10	16.28	Diethyl Phthalate	222.24	$C_{12}H_{14}O_4$	6.17	Phthalate
12	17.07	Benzophenone	182.22	$C_{13}H_{10}O$	2.92	Benzophenones
15	19.91	Hexadecanoic acid, methyl ester	270.45	$C_{17}H_{34}O_2$	1.56	Fatty acid methyl esters
19	21.82	Phytol	296.53	$C_{20}H_{40}O$	11.21	Diterpene alcohol

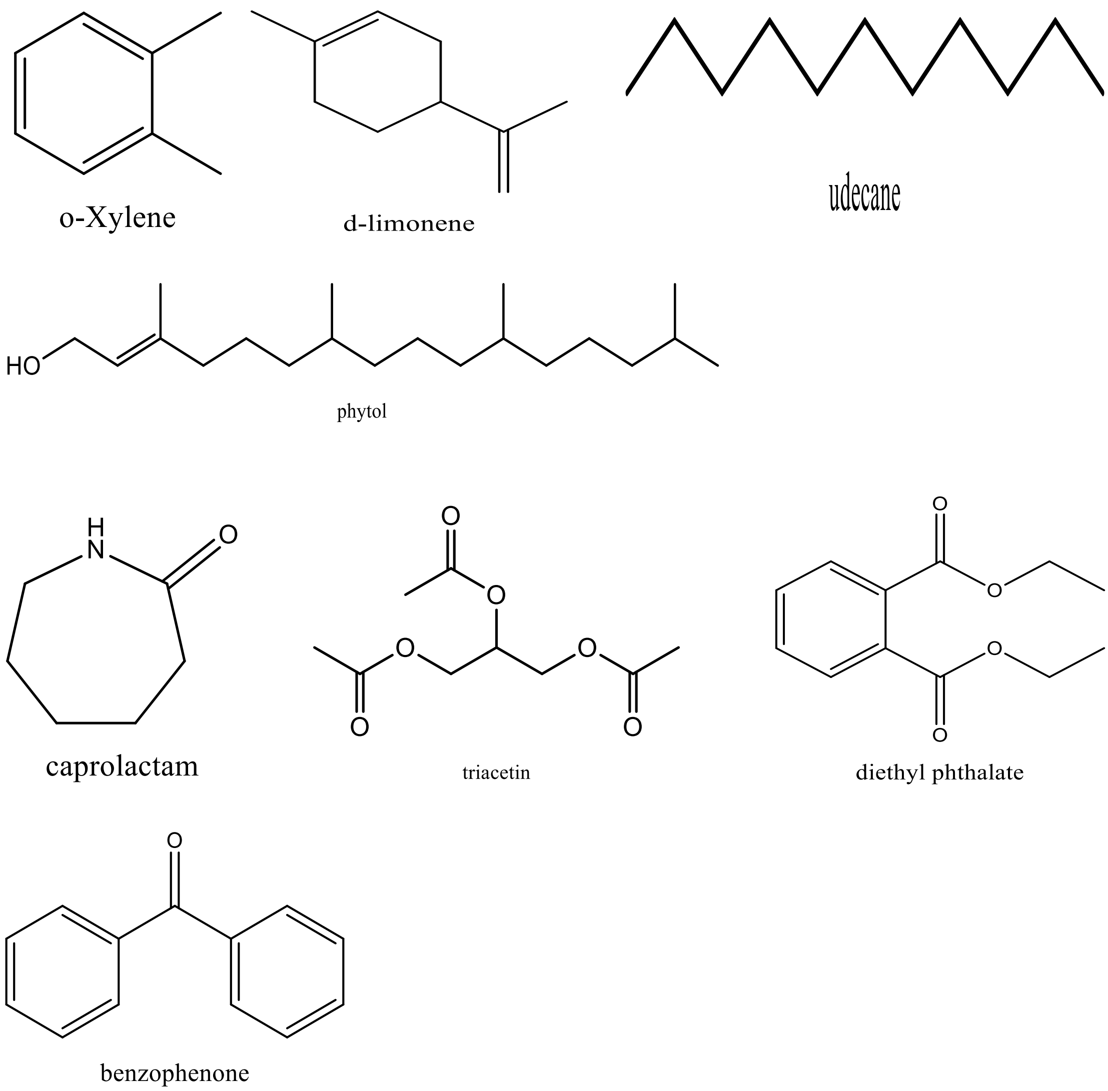

Figure 4.6: Some of the isolated compounds of *Entada abyssinica* leaf extracts

Table 4.4: The list of some secondary metabolites of *Warburgia ugandensis* leaf extracts obtained from GC-MS technique with the reference of NIST 17 spectra information database

S.NO	RT	Name of the compound	Molecular weight	Molecular Formula	% Peak area	Class
1	5.29	Styrene	104.15	C_8H_8	14.60	Hydrocarbon
2	8.74	Undecane	156.31	$C_{11}H_{24}$	1.86	Alkanes
3	10.30	Cyclopropane	42.08	C_3H_6	0.72	Cycloalkane
5	16.36	Caryophyllene oxide	220.35	$C_{15}H_{24}O$	1.29	Sesquiterpenes
6	16.73	Corymbolone	236.35	$C_{15}H_{24}O_2$	2.98	Essential oil
9	17.42	Isoshyobunone	58.12	C_4H_{10}	0.51	Sesquiterpenoids
10	17.68	Patchouli alcohol	222.36	$C_{15}H_{26}O$	1.19	Tertiary alcohol
11	17.74	Aristolene epoxide	204.36	$C_{15}H_{24}O$	1.51	Essential oil

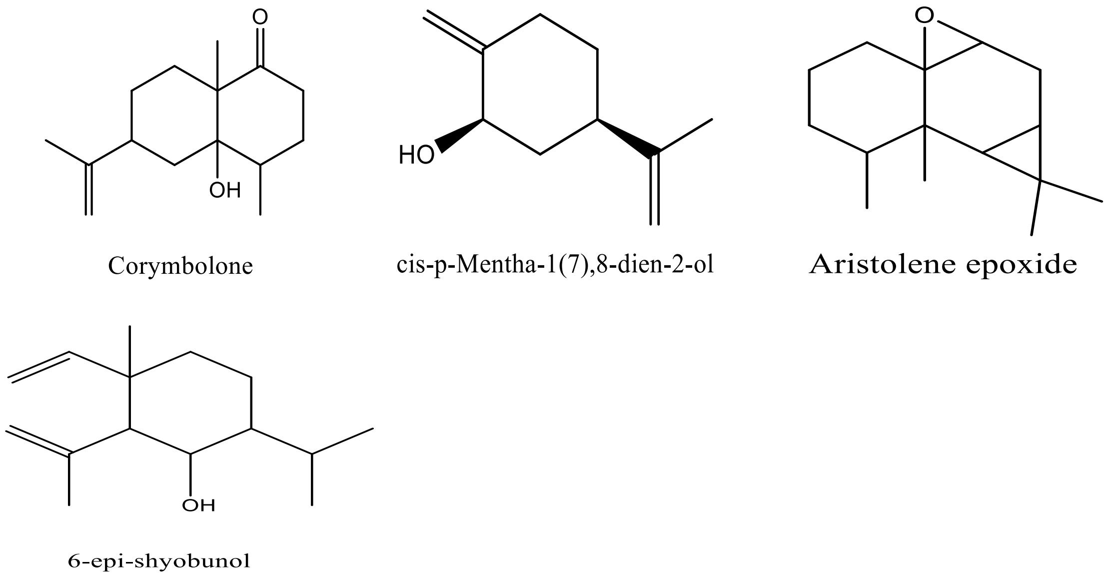

Figure 4.7: Some of the isolated compounds of *Warburgia ugandensis* leaf extracts

4.4 Copper Oxide Nanoparticles synthesized using EA and WU leaf extracts

The synthesis of the NPs was confirmed by visual and spectrophotometric methods. The first characterization step was visual color changes observed as a result of the formulation of nanomaterials as documented in *Flowchart 1*. The formation of copper oxide nanoparticles was confirmed by a light green color from initial blue color of cupric nitrate (Tri-hydrate). This indicated the reduction of Cu^{2+} ions into CuO nanoparticles using aqueous extracts of *Entada abyssinica.* This is similar to a study by Approach *et al*. (Approach *et al*., 2018) that the synthesized CuO nanoparticles are confirmed by color change from blue to sea green by reacting copper acetate solution with flower extracts of *Hibiscus rosa-sinensis.*

During the synthesis process (Amer & Awwad, 2021), the formation of copper oxide nanoparticles was indicated by the observation of brown color from the initial blue color of the Cu $(NO_3)_2$. H_2O solution as a result of the reduction of Cu ions (Cu^{2+} to Cu^o).

In contrast, a review by Hasan & Singh (Hasan & Singh, 2019) also reports that green synthesized copper oxide nanostructures by the reaction of cupric nitrate (tri-hydrate) with plant extracts, dark brown color was formed from the initial blue color of cupric nitrate solution. The color change indicated formation of copper oxide nanomaterials.

(i) (ii) (iii) (iv)

Flowchart 1: Graphical synthesis of copper oxide nanoparticles: (i) Leaf extract, (ii) Cupric nitrate (0.01 M), (iii) plant extract + Cupric nitrate at 50°C -60°C for 45 min and (iv) Cleaned CuO NPs

4.5 Characterization of synthesized CuO NPs

4.5.1 UV-Visible Spectroscopy Analysis of CuO NPs

The optical properties of CuO NPs synthesized using *Entada abyssinica* leaf extracts (*Figure 4.8*) were obtained at wavelengths ranging from 190 nm to 1100 nm. The spectrum of CuO NPs shown the maximum SPR (surface plasmon resonance) peak located at 309.5 nm at pH 6.5 (*Figure 4.8 (a)*), that was a blue-shift to a wave-length of 295.5 nm at high pH of 10.5. At the variation duration of biosynthesis, CuO nanostructures absorbed at a maximum SPR peak of 308 nm after 20 mins at pH 6.5 (*Figure 4.8 (b)*). All the optically characterized absorbance peaks were in similar orientation which further confirmed that the green synthesized nanomaterials were stabilized and also confirmed their purity(Agarwal *et al.*, 2017). In both conditions of varying pH and duration (time) of synthesis, CuO nanoparticles experienced blue shifts. The Tauc's plot in *Figure 4.8 (c)* shows that the CuO nanoparticles possess a higher band gap energy of 3.31 eV at pH 6.5 due to quantum imprisonment or confinement effects (Ijaz *et al*., 2017).

Jayakodi reports green synthesized CuO NPs maximum absorbance peak located at 298 nm and that the increased band-gap energy was due to quantum confinement effects and decrease in particle sizes (Jayakodi, 2020). The sizes of the nanomaterials decreases as the absorption shifts to higher energy or lower wavelengths (blue shifts) as reported by Kosarsoy-agceli, *et al*. (Dulta, Kosarsoy-agceli, *et al*., 2022). The material will be in crystallite structure when the direct bandgap is higher during optical absorption(Tucker *et al*., 2021).

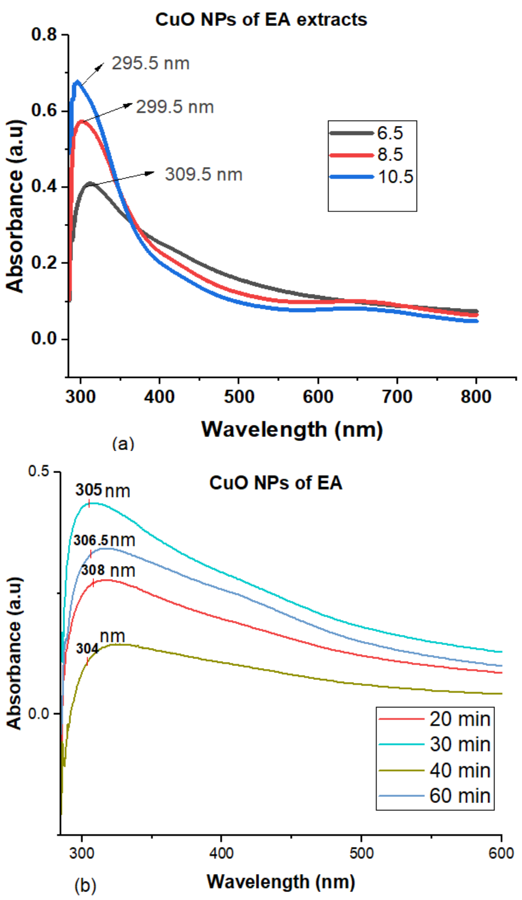

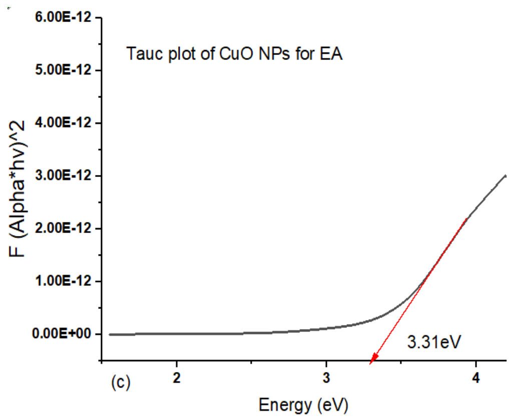

Figure 4.8: UV-Vis absorption spectra for (a) CuO NPs synthesized using *Entada abyssinica* (EA) at varied pH, (b) CuO NPs synthesized using *Entada abyssinica* at varied time and (c) Tauc plot showing band gap of synthesized CuO NPs using *Entada abyssinica*

In (*Figure 4.9 (a)* and *(b)*), the absorption spectra of CuO NPs synthesized from *Warburgia ugandensis* leaf extracts shows maximum optical absorbance peaks at 307.5 nm and 307 nm at varied pH and time respectively. This confirmed the formation of copper oxide nanomaterials. The CuO NPs as shown in tauc's plot (*Figure 4.9 (c)*) had a band-gap energy of 3.24 eV at pH 8.5. A blue shift of 293 nm at pH 10.5 was observed from 304.5 nm at pH 6.5 while a red shift of 307 nm at 40 minutes from initial 295 nm at 30 min at pH 6.5 was observed. This clearly confirmed that with passage of time, there resulted peak broadening and red shifting. The optical results obtained in this thesis agrees with previous results from other studies that the maximum wavelength of CuO NPs was in the range of 285 nm to 330 nm (Joshi, 2019). The SPR (surface plasmon resonance) of CuO nanomaterials results from electromagnetic irradiations which excites electrons freely oscillating in the conduction band. CuO NPs act as semiconductors (Makeswari, 2018). The blue shifts observed can be attributed to decreased nanoparticle sizes (Gebremedhn *et al.*, 2019a).

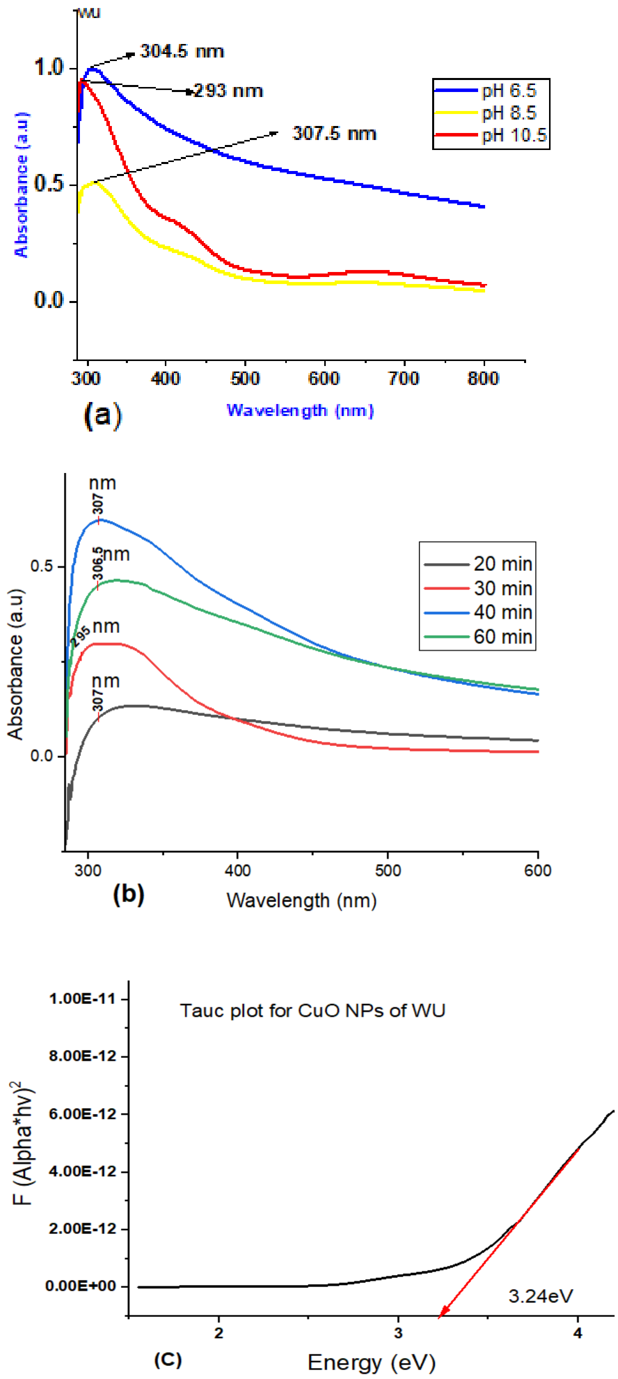

Figure 4.9: UV-Vis absorption spectra for (a) CuO NPs synthesized using *Warburgia ugandensis* (WU) at varied pH, (b) CuO NPs synthesized using *Warburgia ugandensis* at varied time and (c) Tauc plot showing band gap of CuO NPs synthesized using *Warburgia ugandensis*

4.5.2 Fourier-transform infrared Spectroscopy Analysis of CuO NPs

The analysis using FTIR also reinforced the results. The scan range was 400–4000 cm^{-1}. The fingerprinting bands are shown in (Figure 4.10) for CuO NPs synthesized using leaf extracts of *Entada abyssinica*. The stretches of Cu-O was signified by a major peak at 701 cm^{-1} (Figure 4.10) that is in agreement with the results of a study by Gebremedhn *et al*. (Gebremedhn *et al*., 2019b). The bands at 3315 cm^{-1} was assigned to (O-H bond stretching) (Basit *et al*., 2023). The sharp absorption band at 1598 cm-1 can be assigned to C=O ketonic group (indicating presence of flavanones) that unreacted and adsorbed on copper oxide NPs (Sutradhar *et al*., 2014).

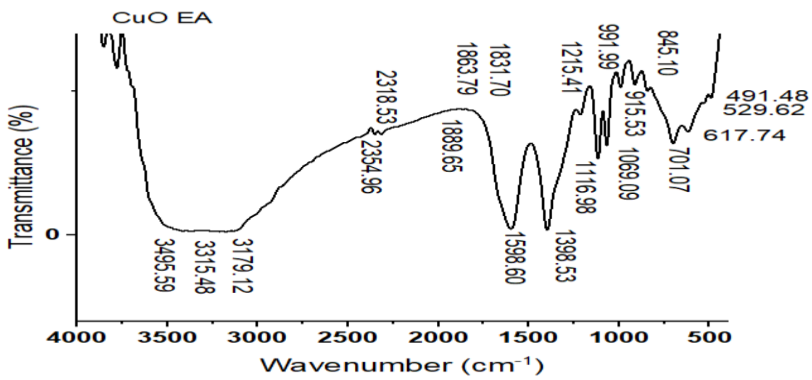

Figure 4.10: FTIR spectrum of CuO NPs synthesized usig *Entada abyssinica* leaf extracts

The small, low frequency sharp bands observed at 616 cm^{-1} and 526 cm^{-1} (*Figure 4.11)* of CuO NPs synthesized using *Warburgia ugandensis* leaf extracts were as a result of Cu-O stretching bonds (indication of CuO NPs formation) and the band at a wavenumber 3421 cm^{-1}-3179 cm^{-1} relates to –OH stretching bonds of phenols, alcohols and adsorbed H_2O (water) molecules (Naga *et al*., 2019), (Jayakodi, 2020), (Alhalili, 2022), (Erci *et al*., 2020). A band located at 1398 cm^{-1} and 3421 cm^{-1} corresponds to N-O bends of nitro and N-H stretches of amides (Dulta, Ko, *et al*., 2022). The C-N stretching at 1115 cm^{-1} correlates to aliphatic (amine) groups

(Jayakodi, 2020). The peak at 1598 cm^{-1} was assigned to C-OH bending vibrations of amides and proteins (Al-fa *et al*., 2021).

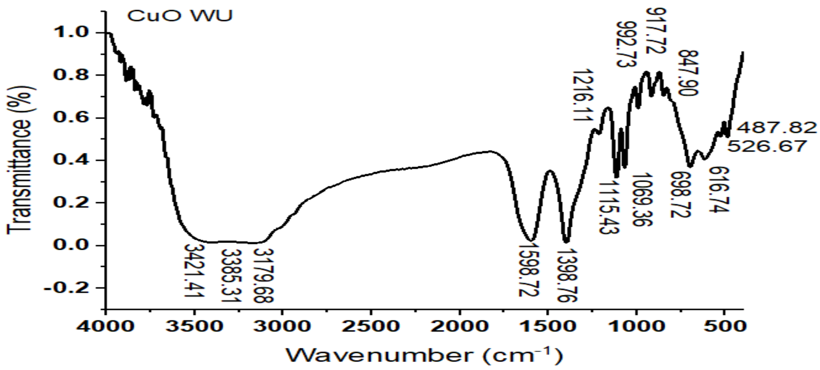

Figure 4.11: FTIR spectrum of CuO NPs synthesized using *Warburgia ugandensis* leaf extracts

4.5.3 X-Ray powder Diffraction (XRD) Spectral Analysis of CuO NPs

The Scherrer's equation was adopted to calculate the particle sizes of the green synthesized CuO and ZnO nanoparticles. The Scherrer's equation (*Equation 1*) was applied as follows;

$$x = \frac{t\lambda}{\beta \sin\theta} \ldots\ldots \textit{Equation 1.}$$

Where;

x=crystallites' average size in nm,

λ=the x-ray radiations' wavelength,

t=shape factor (Scherrer constant usually approximately 0.94)

β =FWHM (width line at half maximum-height in radians) and

θ= (Maximum Peak Diffraction' Position) Bragg's angle (Sorbiun *et al*., 2018), (Chowdhury *et al*., 2020).

For CuO NPs synthesized from *Warburgia ugandensis* extracts (*Figure 4.12*), the sharp peaks diffracted at 32.2°, 39.7° and 61.2° according to JCPDS card NO: 87-

0717, are indexed (111), (200) and (220) respectively. This confirmed that the monoclinic structure of CuO nanoparticles. The purity of the CuO synthesized from *Warburgia ugandensis* extracts was confirmed by absence of other phases. The X-Ray Diffraction shown the crystal nature of CuO NPs (Dulta, Ko, et al., 2022). The XRD pattern also shows diffracted peaks of 2 theta values located at 34.0°, 36.6° and 39.7° indexed to miller indices of 1 1 0, 1 1–1 and 1 1 1 respectively (*Figure 4.12*). In agreement with JCPDS Card NO: 96–901- 5925, the CuO NPs are monoclinic structurally (Ramzan *et al*., 2020). The higher crystallinity in the nanomaterials is indicated by the availability of peaks that are high and sharp in intensity (Ansari *et al*., 2020). The average particle size of CuO nanoparticles obtained was 12.86 nm (*Table 4.5*).

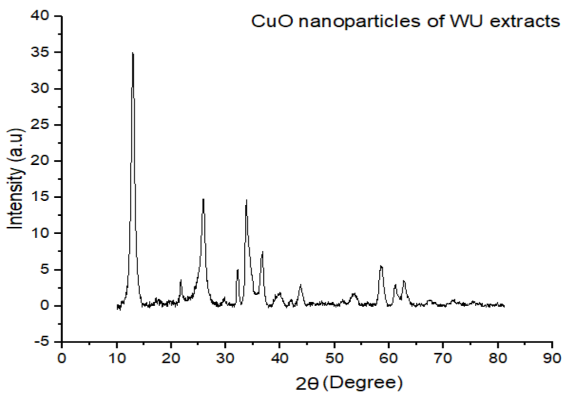

Figure 4.12: XRD pattern of biosynthesized CuO nanoparticles using WU leaf extracts

Table 4.5: Copper oxide nanoparticles synthesized using WU leaf extracts XRD-Gaussian simulated data

Peak No	**2θ Values (°)**	**Full Width Half Maximum (FWHM)**	**Particulate sizes (0.9*0.154)/$(\beta \sin \theta)$(nm)**
1	12.94	0.72	11.12
2	21.79	0.44	18.22
3	25.81	0.98	8.32
4	32.20	0.36	23.00
5	33.96	0.86	9.67
6	36.63	0.64	13.01
7	39.72	0.94	8.97
8	43.75	0.62	13.86
9	53.52	0.90	9.85
10	58.57	0.72	12.56
11	61.20	0.60	15.27
12	62.79	0.78	11.88
Averaged Particle size (nm)			**12.86**

Using Debye Scherrer's equation, the calculated average particle size of CuO nanoparticles was 9.09 nm (*Table 4.6*). As demonstrated in *Figure 4.13*, the XRD pattern of CuO NPs synthesized from *Entada abyssinica* leaf extracts shows peaks located 32.2°, 34.0°, 39.4°, 53.5°, 58.5° and 62.9° which are indexed (110), (002), (111), (020), (202) and (113) respectively. This confirmed that the synthesized CuO nanoparticles were monoclinic in nature which is in accordance with (JCPDS card no.

801268) and (JCPDS card no. 801916) standards (Qamar *et al*., 2020), (Andualem *et al*., 2020).In addition, the peaks observed at 25.1° and 43.8° corresponds to (012) and (220) reflections respectively. This indicated the formation of typical monoclinic CuO NPs which agrees with (JCPDS card no: 48- 1548) (Begum *et al*., 2020).

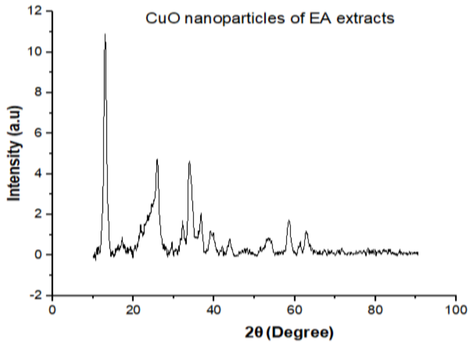

Figure 4.13: XRD pattern of biosynthesized CuO nanoparticles using EA leaf extracts

Table 4.6: Copper oxide nanoparticles synthesized using EA leaf extracts XRD-Gaussian simulated data

Peak No	2θ (°) Values	Full Width Half Maximum (FWHM)	Particulate sizes (0.9*0.154)/(β $\sin\theta$)(nm)
1	12.98	0.73	11.00
2	25.11	2.96	2.75
3	32.18	0.69	11.90
4	34.04	1.04	7.95
5	36.53	1.12	7.47
6	39.42	1.10	7.64
7	43.82	0.63	13.65
8	53.47	1.33	6.70
9	58.53	0.80	11.34
10	62.94	0.89	10.48
Averaged Particle size (nm)			**9.09**

4.6 Zinc Oxide Nanoparticles synthesized of using EA and WU leaf extracts

The observation of a yellowish color indicated the biosynthesis of zinc oxide nanoparticles as shown in *Flowchart 2.* A similar color change (brown to pale yellow) was observed on the green fabrication of ZnO nanoparticles using *Magnoliae officinalis* aqueous leaf extracts (Karkhane & Marzban, 2020). The study by (Mahalakshmi *et al*., 2020) which synthesized ZnO nanoparticles from *Sesbania grandiflora* leaf extracts and zinc acetate solution, the formation of zinc oxide nanoparticles was indicated by the formation of a pale-yellow paste in color.

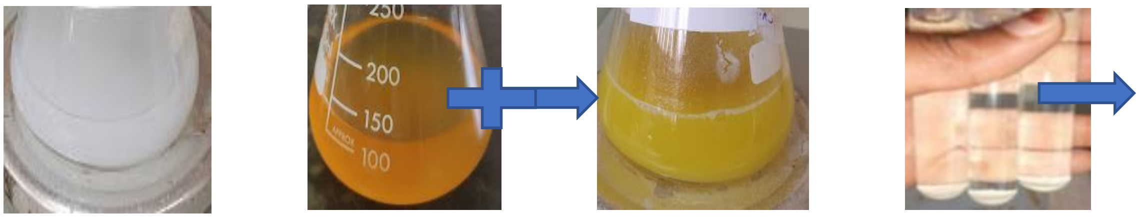

(i) (ii) (iii) (iv)

Flowchart 2: Graphical synthesis of zinc oxide nanoparticles: (i) Zinc acetate solution (100 mM), (ii) leaf extracts, (iii) plant extract + zinc acetate at 50°C - 60°C and (iv) Cleaned ZnO NPs

4.7 Characterization of synthesized ZnO NPs

4.7.1 UV-Visible Spectroscopy Analysis of ZnO NPs

The optical characteristics of the biosynthesized zinc oxide nanoparticles using leaf extracts of *Warburgia ugandensis* dispersed in distilled water were carried out where the spectrum of absorption was obtained using a double beam UV-Vis spectrophotometer (SHIMADZU model) at a range of 190-1100 nm wavelength scan. The maximum absorption peak of ZnO nanoparticles synthesized from leaf extracts of WU (*Figure 4.14*) was obtained at 362.5 nm after 30 minutes at a pH of 11. The surface plasmon resonance peak at varied time shifted to 365.5 nm after 60 minutes from initial 367 nm at 40 mins at pH of 8. The blue shift of 365.5 nm at 60 minutes and a red shift of 362.5 nm at pH 11 observed could be attributed by decrease and increase in particle sizes respectively (Ifeanyichukwu & Fayemi, 2020), (Ravichandran *et al*., 2020).

The band gap energy obtained from Tauc plot was 2.53 eV at pH 11. This was consistent with a study applying water hyacinth and mango steen peels crude extracts to synthesize ZnO nanoparticles (T-thienprasert, 2022), where the absorbance peak was located at 365 nm and a band gap of 2.88 eV. Furthermore, the spectra do not contain other peaks signifying that the green synthesized nanoparticles were a pure product. The higher absorption peaks of 367 nm as reported by (Abdelbaky *et al*., 2022) can be attributed by inherent band gap absorptions by ZnO's as electrons transition to conduction band (Ec) from valence band (Ev).

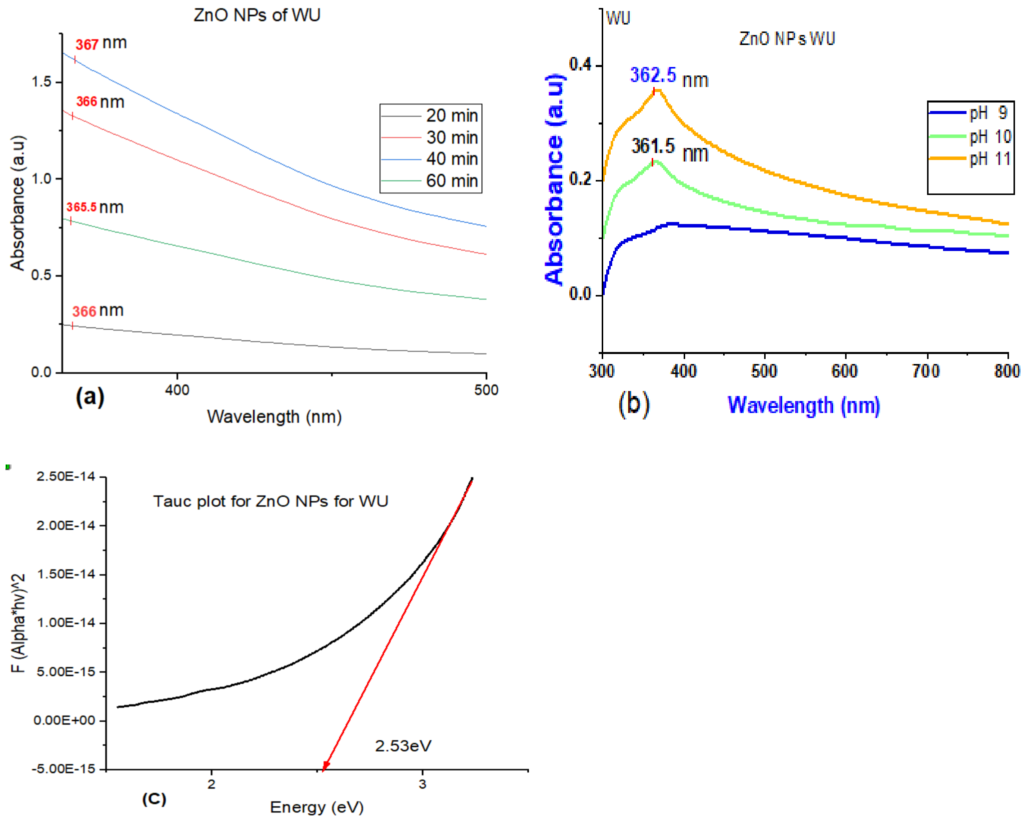

Figure 4.14: Absorption spectra for (a) ZnO-NPs synthesized using *Warburgia ugandensis* (WU) at varied time, (b) ZnO-NPs synthesized using *Warburgia ugandensis* (WU) at varied pH and (c) Tauc plot showing band gap for the synthesized ZnO NPs using *Warburgia ugandensis* (WU)

For ZnO NPs synthesized using leaf extracts of *Entada abyssinica* (EA) (*Figure 4.15 (a) and (b)*), the optical absorbance peaks at higher wavelengths appeared at 364.5 nm and 359.5 nm at varied pH and time respectively. The maximum absorbance wavelength of zinc oxide nanoparticles lies in the range of 355 nm to 380 nm (Rahman *et al*., 2022). At varied pH, the absorption peaks show a blue shift while at varied time of synthesis, a red shift of 359.5 nm appeared at 60 min. The blue shift absorbance excitations resulted from a decrease in particle sizes and an indication of quantum imprisonment effects of nanoparticles (J. Singh *et al*., 2019). At pH 9, there was no absorbance peak observed as was also reported by Mutukwa & Taziwa (Mutukwa & Taziwa, 2022) that at pH between 8-10, no surface plasmon resonance absorbances were observed. It was linear revealing that the ZnO NPs formation was ideal or favorable at alkalinity of above pH 9.

The tauc plot of ZnO NPs (*Figure 4.15 (c)*) shown a band gap energy of 2.84 eV at pH 10.5 which is similar to results reported by (Muthukumaran *et al*., 2018). The green fabricated NPs are spherical in shape in accordance with Mei's theory stating that: ‘’ The shape of the synthesized nanoparticle is spherical if a single sharp absorbance peak was observed in the UV–Vis spectrum’’ (Maduabuchi *et al.*, 2019).

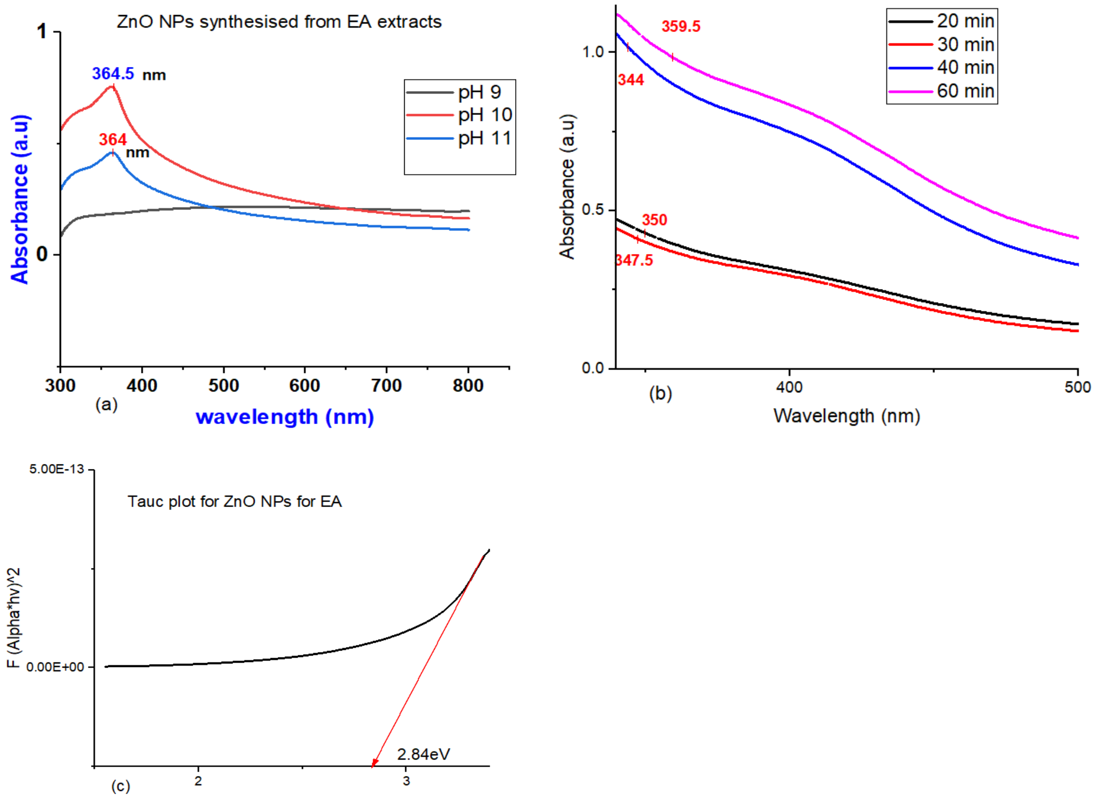

Figure 4.15: UV-Vis absorption spectra for (a) ZnO NPs synthesized using *Entada abyssinica* at varied pH, (b) ZnO NPs synthesized using *Entada abyssinica* at varied time and (c) Tauc plot showing band gap of synthesized ZnO NPs using *Entada abyssinica*

4.7.2 Fourier-transform infrared Spectroscopy Analysis of ZnO NPs

The scan range was 400–4000 cm^{-1}. The fingerprints and different peak areas are shown in (Figure 4.16) for ZnO NPs synthesized using leaf extracts of *Entada abyssinica*. The Zn-O stretching vibration was indicated at 549 cm^{-1} and 453 cm^{-1} as was similarly reported by Sutradhar & Saha (Sutradhar & Saha, 2016) that biosynthesized ZnO nanoparticles' characteristic peak was located at 530 cm^{-1}. It was also reported that the green synthesized ZnO-NPs displayed their absorption peaks at the wavelengths of 485 cm^{-1} , 450 cm^{-1}, 436 cm^{-1} and 442 cm^{-1} ranging between 400-500 cm^{-1} ((Abdelbaky *et al*., 2022),(Aklilu, 2022)). Therefore, it was consistent with other findings. The functional groups responsible for the reduction, capping and stabilization of the green synthesized ZnO NPs using *Entada abyssinica* were shown at 3020 cm^{-1} (C-H bond Stretching), 1647 cm^{-1} (C=C bond stretching) and 1737 cm^{-1} (C=O bond stretching) (Nagarajan, 2017), (Mohamed, 2020). The bands at 3387cm^{-1} was assigned to (O-H bond stretching) (Basit *et al*., 2023).

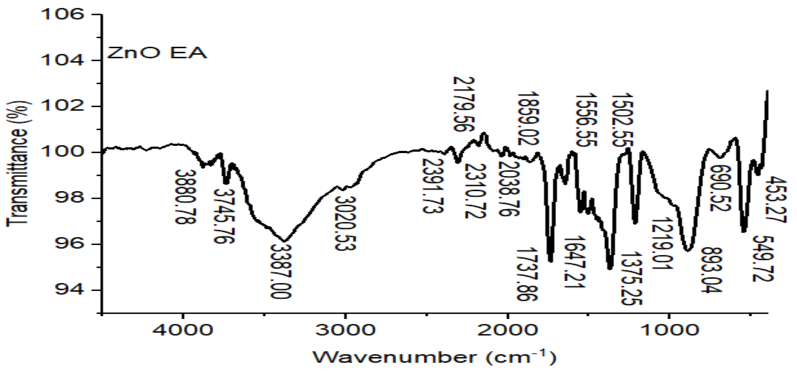

Figure 4.16: FTIR spectrum of ZnO NPs synthesized using *Entada abyssinica* leaf extracts

Figure *4.17* identifies the bands of various functional groups present in *Warburgia ugandensis* leaf extracts that are responsible for the formation of ZnO NPs. This was also reported in QC-MS analysis. The broad peak at 3003 cm^{-1} can be attributed to C-H and –CH_2 bending bonds of alkenes. The peak at 1647 cm^{-1} was assigned to C-OH bending vibrations of amides, proteins or carboxylate acids (Al-fa *et al*., 2021). In *Figure 4.17*, the bands that absorbed at lower wavenumbers ranging from 400 cm^{-1} - 600 cm^{-1} indicated existence of Zn-O bonds in the green formulated ZnO nanoparticles (Muthukumaran *et al*., 2018),(Awwad *et al*., 2020) (Uyen *et al*., 2020), (El-belely *et al*., 2021). Therefore, the stretching at 543 cm^{-1} shows the formation of ZnO NPs. The current study discovered that the FTIR bands substantiated the presence of alkyl, alkenes, ketones, aldehydes, carboxylic acids, phenols and alcohols responsible for the bio-reduction, encapsulation and stabilization of the green synthesized nanoparticles.

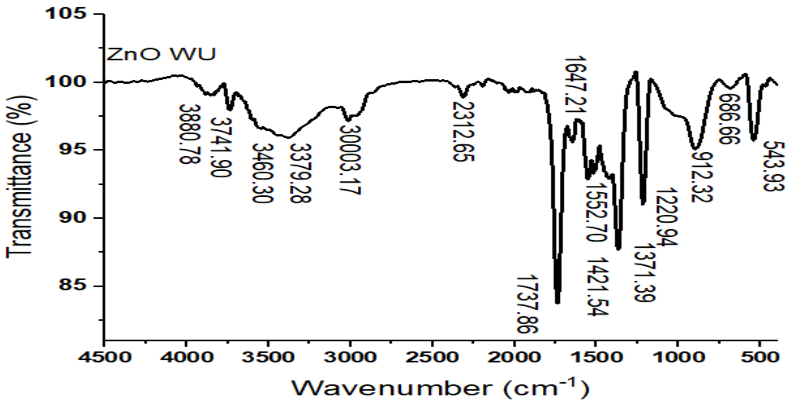

Figure 4.17: FTIR spectrum of ZnO NPs synthesized using *Warburgia ugandensis* leaf extracts

4.7.3 X-Ray powder Diffraction (XRD) Spectral Analysis of ZnO NPs

The Bragg's 2θ values for ZnO NPs (*Figure 4.18*) were located at 31.8°, 34.4°, 36.3°, 47.5°, 56.6°, 62.8°, 68.0° and 69.1°. These peaks as reported by (Abdelbaky *et al*., 2022), (Midatharahalli *et al*., 2019) and (Faisal *et al*., 2021), corresponds to miller indices of (100), (002), (101), (102), (110), (103), (112) and (201) respectively. This is in accordance to (JCPDS card No: 36-1451), JCPDS CARD No: 80-0075, ICSD card No: 067849 and JCPDS card NO 36 -1451. This was an indication that the obtained ZnO nanoparticles are pure hexagonal wurtzite structures. The average particle size obtained from Scherrer's equation for ZnO nanoparticles was 21.2 nm (*Table 4.7*).

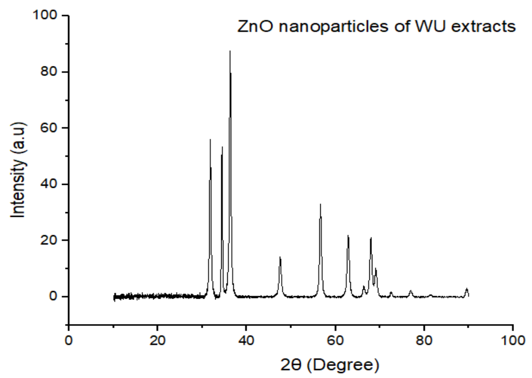

Figure 4.18: XRD pattern of biosynthesized ZnO nanoparticles using WU leaf extracts

Table 4.7: Zinc oxide nanoparticles synthesized using WU leaf extracts XRD-Gaussian simulated data

Peak No	2θ Values (°)	Full Width Half Maximum (FWHM)	Particulate sizes $(0.9*0.154)/(\beta \sin\theta)$(nm)
1	31.77	0.35	23.36
2	34.40	0.24	34.02
3	36.26	0.38	22.07
4	47.53	0.52	16.73
5	56.60	0.45	19.91
6	62.84	0.51	18.09
7	67.95	0.52	18.54
8	69.06	0.57	16.93
Averaged Particle size (nm)			**21.21**

Figure *4.19* shows the ZnO NPs XRD spectrum peaks synthesized from *Entada abyssinica* leaf extracts to confirm its crystallinity. The 2θ values diffracted at 31.8°; 34.4°; 36.3°; 47.6°; 56.6°; 62.9°; 68.0° and 69.1° corresponds to 100, 002, 101, 102, 110, 103, 112 and 201 respectively. This confirms that the biosynthesized ZnO NPs were polycrystalline hexagonal Wurtzite in shape in accordance with JCPDS Card NO: 5-0664 and JCPDS Card NO: 00-065-3411 (Lopez-miranda *et al*., 2023), (Fouda *et al*., 2020). From the XRD spectroscopy data, the obtained average particle size for ZnO NPs was 24.36 nm (*Table 4.8).* The sharpness of the spectrum peaks indicates that the nanoparticles are found within nanoscale range (Radhakrishnan *et al.*, 2021) and stabilization carried out by bio-reducing molecules of *Entada abyssinica* leaf extracts.

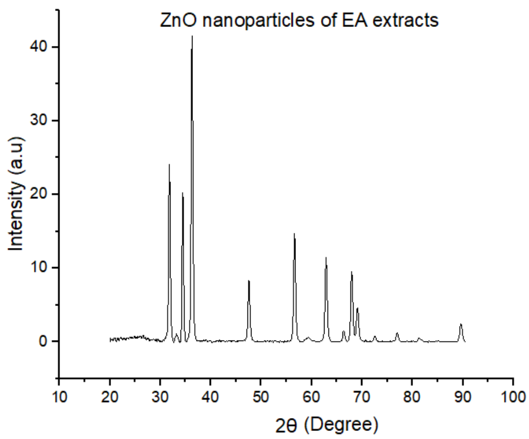

Figure 4.19: XRD pattern of biosynthesized ZnO nanoparticles using EA leaf extracts

Table 4.8: Zinc oxide nanoparticles synthesized using EA leaf extracts XRD-Gaussian simulated data

Peak No	2θ Values (°)	Full Width Half Maximum (FWHM)	Particulate sizes $(0.9*0.154)/(\beta \sin\theta)$(nm)
1	31.80	0.34	24.39
2	34.45	0.29	28.68
3	36.28	0.34	24.63
4	47.57	0.38	22.78
5	56.62	0.38	23.54
6	62.88	0.41	22.96
7	67.96	0.41	23.19
8	69.09	0.45	21.53
9	76.97	0.37	27.61
10	89.62	0.46	24.29
Averaged Particle size (nm)			**24.36**

4.8 Antimicrobial Activity

The antimicrobial activity of CuO and ZnO nanoparticles synthesized from *Entada abyssinica* and *Warburgia ugandensis crude* extracts, *Entada abyssinica* and *Warburgia ugandensis* crude extracts and ampicillin were studied against Gram negative bacteria (*Escherichia coli*) and Gram positive (*Staphylococcus aureus*) bacteria by agar disc diffusion technique. The results obtained are as shown in *Figure 4.20: (i)* to *(XiV)* and *Table 4.9.* Amongst the test samples studied, CuO Nps synthesized using EA leaf extracts showed to be more sensitive towards Gram positive bacteria (*Staphylococcus aureus*) with the zone of inhibition (ZOI) of 12.0±1.0 mm. It also displayed more sensitivity towards Gram negative bacteria (*Escherichia coli*) with the ZOI of 11.3±1.2 mm (Figure 4:20). The antibacterial effectivity of ampicillin as a positive control was studied against the two bacterial strains: *Escherichia coli* and *Staphylococcus aureus* exhibiting zones of inhibition of 9.0±1.0 mm and 9.3±0.6 mm respectively (Figure 4:20).

ZnO Nps synthesized using WU leaf extracts showed more sensitivity towards Gram negative (*Escherichia coli*) bacteria with a ZOI of 9.6±1.5 mm than Gram positive (*Staphylococcus aureus*) bacteria with the zone of inhibition of 9.0±1.0 mm (Figure 4:20). *Escherichia coli* bacteria showed less sensitivity towards CuO NPs synthesized using WU leaf extracts displaying a zone of inhibition of 7.3±0.6 mm (Figure 4:20). This implies that *Escherichia coli* bacteria seemed highly resistant. As documented by Shigwenya *et al*., the difference in the inhibition of bacteria growth was as a result of the difference of their thickness of cell walls (Shigwenya *et al.*, 2020). Therefore, in this present study of biosynthesis of CuO and ZnO nanoparticles for biological applications for the first time shown positive results. This was because it was confirmed that the bio-formulated nanoparticles and the phytochemicals present possessed more antimicrobial activity. As reported by Ssekatawa *et al.*, the morphology of NPs affects bactericidal activities. The rod-shaped nanostructures have larger surface-area-to-volume ratios resulting in growth inhibition of bacteria due to increased interactions. The positively charged green synthesized nanoparticles attracts the negatively charged cell walls of microbes caused by electro-static forces, adsorptions and finally degeneration of microbial membranes (Ssekatawa *et al*., 2022). A similar study by Journal *et al.* reports that the bactericidal activities are not fully clear. The following mechanisms were documented: (i) The replications of DNA get impaired and decreased intra-cellular ATP levels. (ii) The release of ROS (reactive oxygen species) cause oxidative stress that cause oxidative denaturation of cell membranes. (iii) When the nanostructures accumulate and dissolve in the membranes of bacteria, the permeability is changed (dissipating proton motive force in the plasma membrane) and releasing intra-cellular molecules (membrane proteins and lipopolysaccharides) (Journal *et al.*, 2020).

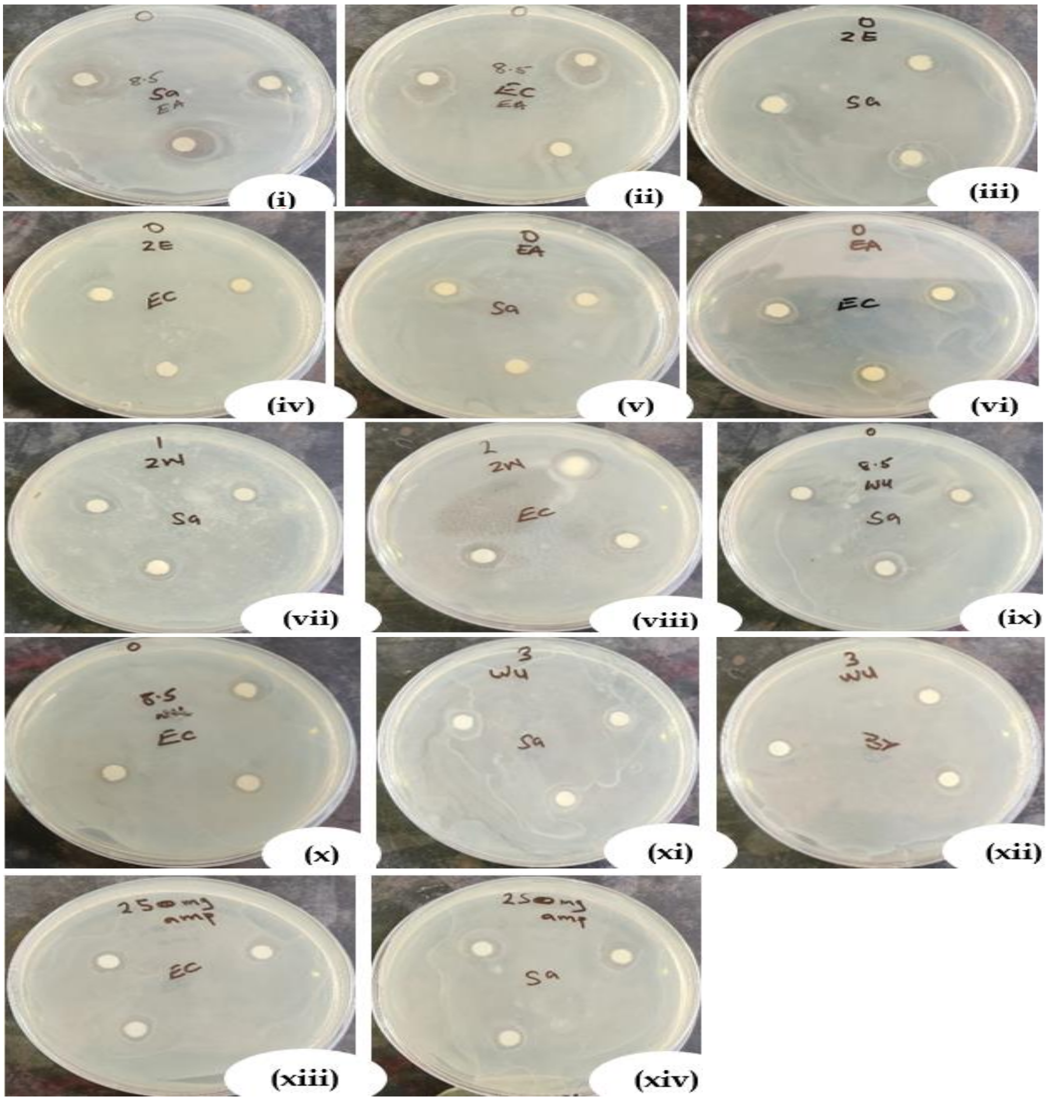

Figure 4.20: (i) Petri dish representing zone of inhibition by biosynthesized CuO NPs of Entada abyssinica extracts against: (i) Staphylococcus aureus and (ii) Escherichia coli, Petri dish representing zone of inhibition by biosynthesized ZnO NPs of Entada abyssinica extracts against: (iii) Staphylococcus aureus and (iv) Escherichia coli, Petri dish representing zone of inhibition by Entada abyssinica extracts against: (v) Staphylococcus aureus and (vi) Escherichia coli, Petri dish representing zone of inhibition by biosynthesized ZnO NPs of Warburgia ugandensis extracts against: (vii) Staphylococcus aureus and (viii) Escherichia coli, Petri dish representing zone of inhibition by biosynthesized CuO NPs of Warburgia ugandensis extracts against: (ix) Staphylococcus aureus and (x) Escherichia coli, Petri dish representing zone of inhibition by Warburgia ugandensis extracts against: (xi) Staphylococcus aureus and (xii) Escherichia coli and Petri dish representing zone of inhibition by ampicillin against: (xiii) Staphylococcus aureus and (xiv) Escherichia coli

Table 4.9: Zones of inhibition of CuO NPs and ZnO NPs synthesized using *Warburgia ugandensis* crude extracts, CuO NPs and ZnO NPs synthesized using *Entada abyssinica* crude extract, *Entada abyssinica* crude extract, *Warburgia ugandensis* crude extract and ampicillin against *S. aureus* and *E. coli*

	Zones of Inhibition (mm)	
Sample Name	***S. aureus***	***E. coli***
CuO NPs of WU	8.3±0.6	7.3±0.6
ZnO NPs of WU	9.0±1.0	9.6±1.5
CuO NPs of EA	12.0±1.0	11.3±1.2
ZnO NPs of EA	10.0±1.0	8.0±1.0
Entada abyssinica extracts	7.3±0.6	8.0±0.0
Warburgia ugandensis extracts	8.0±1.0	8.0±1.0
Ampicillin	9.3±0.6	9.0±1.0

The Zones of Inhibition (mm) are reported as mean ± standard deviation (SD) of the bacterial strains: *S. aureus* (*Staphylococcus aureus*) and *E. coli (Escherichia coli) (Table 4.9).*

4.9 Statistical Analysis-One-Way ANOVA

Table 4.10: The ANOVA analysis of *E. coli* ZOI results

Anova: Single Factor						
SUMMARY						
Groups	*Count*	*Sum*	*Average*	*Variance*		
CuO NPs of WU	3	22	7.333333	0.333333		
ZnO NPs of WU	3	29	9.666667	2.333333		
CuO NPs of EA	3	34	11.33333	1.333333		
ZnO NPs of EA	3	24	8	1		
Entada abyssinica extracts	3	21	7	0		
Warburgia ugandensis extracts	3	22	7.333333	0.333333		
Ampicillin	3	27	9	1		
ANOVA						
Source of Variation	*SS*	*df*	*MS*	*F*	*P-value*	*F crit*
Between Groups	44.57143	6	7.428571	8.210526	0.000609	2.847726
Within Groups	12.66667	14	0.904762			
Total	57.2381	20				

The p-value is less than 0.05 thus the obtained anti-bacterial results are significant.

Table 4.11: The ANOVA analysis of *S. aureus* ZOI results

Anova: Single Factor						
SUMMARY						
Groups	*Count*	*Sum*	*Average*	*Variance*		
CuO NPs of WU	3	25	8.333333	0.333333333		
ZnO NPs of WU	3	27	9	1		
CuO NPs of EA	3	36	12	1		
ZnO NPs of EA	3	30	10	1		
Entada abyssinica extracts	3	22	7.333333	0.333333333		
Warburgia ugandensis extracts	3	24	8	1		
Ampicillin	3	28	9.333333	0.333333333		
ANOVA						
Source of Variation	*SS*	*df*	*MS*	*F*	*P-value*	*F crit*
Between Groups	42.57143	6	7.095238	9.933333333	0.000226	2.847726
Within Groups	10	14	0.714286			
Total	52.57143	20				

The p-value is less than 0.05 thus the obtained anti-bacterial results are significant.

CHAPTER FIVE

CONCLUSION AND RECCOMMENDATIONS

5.1 Conclusion

The phytochemical screening shows that both plant species (*Entada abyssinica* and *Warburgia ugandensis*) possess various secondary metabolites like saponins, phenols, alkaloids, tannins and flavonoids responsible for the formation of the nanoparticles. The quantitative analysis of total contents of specific bioactive constituents and GC-MS analysis, also confirmed the presence of various phytochemicals in *Warburgia ugandensis* and *Entada abyssinica* plant extracts. The two-plant species were found to possess total phenolic contents, total flavonoid contents and total tannins contents in the range of 19-58 mg/g, 940-1400 mg/g and 0.6-4.9 mg/g of the acid equivalents respectively. The total percentage contents of saponins and alkaloids were in the range of 0.94-1.33% and 1.27-1.42% respectively. The green synthesis using plant extracts is a simple and a less costly technique which is environmentally friendly. The biosynthesis of copper oxide and Zinc oxide nanoparticles was successfully achieved using *Entada abyssinica* and *Warburgia ugandensis* leaf extracts inspired synthesis and was reported for the first time in this study. This was confirmed from UV-VIS (Ultra Violet- Visible Spectroscopy), FT-IR (Fourier -Transform -Infrared Spectroscopy) and XRD (X-Ray- Diffraction) characterization techniques used for analysis. The optical characteristics by Ultra Violet-Visible spectrometer (UV-VIS), indicated the successful synthesis of ZnO NPs and CuO NPs from *Warburgia ugandensis* leaf extracts with a maximum peak at 367 nm and 307.5 nm respectively. For ZnO NPs and CuO NPs synthesized using *Entada abyssinica* leaf extracts, the maximum absorptions were observed at 364.5 nm and 309.5 nm respectively. The functional groups of the biomolecules responsible for the reduction, capping and reduction of nanoparticles, the Cu-O bonds (701 cm^{-1} for *Entada abyssinica* and 616 cm^{-1}, 526 cm^{-1} for *Warburgia ugandensis*) and Zn-O bonds (549 cm^{-1}, 453 cm^{-1} for *Entada abyssinica* and 543 cm^{-1} for *Warburgia ugandensis*) characteristic absorbances were confirmed in FT-IR spectra. The XRD pattern utilized in calculation of the average particle sizes has shown that the CuO NPs of *Warburgia ugandensis* and *Entada abyssinica* had 12.86 nm and 9.09 nm respectively. The average particle sizes of ZnO NPs of *Warburgia ugandensis* and *Entada abyssinica* were 21.20 nm and 24.36 nm respectively. The XRD analysis has demonstrated the purity and monoclinic phase of CuO nanoparticles and hexagonal wurtzite structures of ZnO nanoparticles synthesized using *Warburgia ugandensis* and *Entada abyssinica.* The test of the bactericidal activities of the green synthesized nanomaterials was effective. The nanoparticles mostly exist inform of ions which are strong reactive species thus proofed to be excellent antimicrobial agents against the Gram negative (*Escherichia coli*) and Gram-positive (*Staphylococcus aureus*) bacteria during the research work. Therefore, this study concludes that the synthesized nanoparticles can be applied in medicine in the treatment of pathogens causing diseases.

5.2 Recommendations

Green synthesized CuO NPs and ZnO NPs should be applied in the formulation of new bactericidal medicine.

5.3 Recommendations for Further Study

The future research work to be done by the authors is;

1) To carry out the anti-oxidant properties of the biosynthesized CuO nanoparticles and ZnO nanoparticles.

2) To carry out the anti-cancer properties of the biosynthesized CuO nanoparticles and ZnO nanoparticles.
3) To carry out the anti-fungal properties of the biosynthesized CuO nanoparticles and ZnO nanoparticles.
4) The study and characterization of specific phytochemicals which resulted to the reduction, capping and stabilization of CuO nanoparticles and ZnO nanoparticles.
5) The study of exact bactericidal action mechanisms of CuO nanoparticles and ZnO nanoparticles on microbes.
6) The test of green synthesized CuO NPs and ZnO NPs against other potentially MDR (multi drug resistant) bacteria to facilitate their developments into anti-bacteria agents.

REFERENCES

Abdelbaky, A. S., El-mageed, T. A. A., Babalghith, A. O., Selim, S., & Mohamed, A. M. H. A. (2022). *Green Synthesis and Characterization of ZnO Nanoparticles Using Pelargonium odoratissimum (L .) Aqueous Leaf Extract and Their Antioxidant , Antibacterial and Anti-inflammatory Activities*.

Agarwal, H., Kumar, S. V., & Rajeshkumar, S. (2017). Resource-Efficient Technologies Review article A review on green synthesis of zinc oxide nanoparticles – An eco-friendly approach. *Resource-Efficient Technologies*, *3*(4), 406–413. https://doi.org/10.1016/j.reffit.2017.03.002

Ahmad, W., & Kalra, D. (2020). Journal of King Saud University – Science Green synthesis , characterization and anti microbial activities of ZnO nanoparticles using Euphorbia hirta leaf extract. *Journal of King Saud University - Science*, *32*(4), 2358–2364. https://doi.org/10.1016/j.jksus.2020.03.014

Ahmed, B., Syed, A., Ali, K., Elgorban, A. M., Khan, A., Lee, J., & AL-Shwaiman, H. A. (2021). Synthesis of gallotannin capped iron oxide nanoparticles and their broad spectrum biological applications. *RSC Advances*, *11*(17), 9880–9893. https://doi.org/10.1039/d1ra00220a

Akbar, S., Tauseef, I., Subhan, F., Sultana, N., Khan, I., Ahmed, U., & Haleem, K. S. (2020). An overview of the plant-mediated synthesis of zinc oxide nanoparticles and their antimicrobial potential. *Inorganic and Nano-Metal Chemistry*, *50*(4), 257–271. https://doi.org/10.1080/24701556.2019.1711121

Akinseye, O. R. (2017). *Qualitative and Quantitave Evaluation of the Phytochemicals in Dry , Wet and Oil Extracts of the Leaf of Morinda lucida*. *7*(7), 22–25.

Aklilu, M. (2022). *Khat (Catha edulis) Leaf Extract-Based Zinc Oxide Nanoparticles and Evaluation of Their Antibacterial Activity*. *2022*.

Al-fa, A. M., Abu-kharma, M. H., & Awwad, A. M. (2021). *Green synthesis of copper oxide nanoparticles using Bougainvillea leaves aqueous extract and antibacterial activity evaluation*. *7*(3), 155–162.

Algebaly, A. S., Mohammed, A. E., Abutaha, N., & Elobeid, M. M. (2020). Saudi Journal of Biological Sciences Biogenic synthesis of silver nanoparticles : Antibacterial and cytotoxic potential. *Saudi Journal of Biological Sciences*, *27*(5), 1340–1351. https://doi.org/10.1016/j.sjbs.2019.12.014

Alhalili, Z. (2022). Green synthesis of copper oxide nanoparticles CuO NPs from Eucalyptus Globoulus leaf extract : Adsorption and design of experiments. *Arabian Journal of Chemistry*, *15*(5), 103739. https://doi.org/10.1016/j.arabjc.2022.103739

Amer, M. W., & Awwad, A. M. (2021). Green synthesis of copper nanoparticles by Citrus limon fruits extract , characterization and antibacterial activity. *Chemistry International*, *7*(1), 1–8.

Andualem, W. W., Sabir, F. K., Mohammed, E. T., Belay, H. H., & Gonfa, B. A. (2020). *Synthesis of Copper Oxide Nanoparticles Using Plant Leaf Extract of Catha edulis and Its Antibacterial Activity*. *2020*.

Ansari, M. A., Murali, M., Prasad, D., Alzohairy, M. A., Almatroudi, A., Alomary, M. N., Udayashankar, A. C., Singh, S. B., Asiri, S. M. M., Ashwini, B. S., Gowtham, H. G., Kalegowda, N., Amruthesh, K. N., Lakshmeesha, T. R., & Niranjana, S. R. (2020). Cinnamomum verum bark extract mediated green synthesis of ZnO nanoparticles and their antibacterial potentiality. *Biomolecules*, *10*(2), 1–14. https://doi.org/10.3390/biom10020336

Anywar, G., Kakudidi, E., Byamukama, R., Mukonzo, J., Schubert, A., Oryem-Origa, H., & Jassoy, C. (2021). A Review of the Toxicity and Phytochemistry of Medicinal Plant Species Used by Herbalists in Treating People Living With HIV/AIDS in Uganda. *Frontiers in Pharmacology*, *12*(April), 1–10. https://doi.org/10.3389/fphar.2021.615147

Approach, F., Copper, S., Nanoparticles, O., Hibiscus, U., Extracts, F., & Activities, A. (2018). *Biotechniques A Green and Facile Approach for the Synthesis Copper Oxide Nanoparticles Using Hibiscus rosa-sinensis Flower Extracts and It ' s Antibacterial Activities*. *8*(1), 8–11. https://doi.org/10.4172/2155-9821.1000324

Asmira Abd Rahim, E. N., Ismail, A., Omar, M. N., Rahmat, U. N., & Nizam Wan Ahmad, W. A. (2018). GC-MS analysis of phytochemical compounds in syzygium polyanthum leaves extracted using ultrasound-assisted method. *Pharmacognosy Journal*, *10*(1), 110–119. https://doi.org/10.5530/pj.2018.1.20

Awwad, A. M., Amer, M. W., Salem, N. M., & Abdeen, A. O. (2020). *Green synthesis of zinc oxide nanoparticles (ZnO-NPs) using Ailanthus altissima fruit extracts and antibacterial activity*. *6*(3), 151–159.

Baig, N., Kammakakam, I., Falath, W., & Kammakakam, I. (2021). Nanomaterials: A review of synthesis methods, properties, recent progress, and challenges. *Materials Advances*, *2*(6), 1821–1871. https://doi.org/10.1039/d0ma00807a

Basit, R. A., Abbasi, Z., Hafeez, M., Ahmad, P., Khan, J., Khandaker, M. U., Al-mugren, K. S., & Khalid, A. (2023). *Successive Photocatalytic Degradation of Methylene Blue by ZnO , CuO and ZnO / CuO Synthesized from Coriandrum*.

Batool, M., & Mehboob, N. (2018). *L UPINE PUBLISHERS Degradation of Malachite Green by Green Synthesized Copper Nanoparticles by Using Aloe Barbadensis Leaf Extracts*. *1*(2), 29–34. https://doi.org/10.32474/ANOAJ.2018.01.000108

Bayat, M., Chudinova, E., Zargar, M., Lyashko, M., Louis, K., & Adenew, F. K. (2019). Phyto-assisted green synthesis of zinc oxide nanoparticles and its antibacterial and antifungal activity. *Research on Crops*, *20*(4), 725–730. https://doi.org/10.31830/2348-7542.2019.107

Begum, S. N., Esakkiraja, A., Asan, S. M., Muthumari, M., & Raj, G. V. (2020). *Green Synthesis of Copper Oxide Nanoparticles Using Catharanthus Roseus Leaf Extract and Their Antibacterial Activity Green Synthesis of Copper Oxide Nanoparticles Using Catharanthus Roseus Leaf Extract and Their Antibacterial Activity*. *December*.

Bhavyasree, P. G., & Xavier, T. S. (2020). Heliyon Green synthesis of Copper Oxide / Carbon nanocomposites using the leaf extract of Adhatoda vasica Nees , their characterization and antimicrobial activity. *Heliyon*, *6*(January), e03323. https://doi.org/10.1016/j.heliyon.2020.e03323

Biegański, P., Szczupak, Ł., Arruebo, M., & Kowalski, K. (2021). Brief survey on organometalated antibacterial drugs and metal-based materials with antibacterial activity. *RSC Chemical Biology*, *2*(2), 368–386. https://doi.org/10.1039/d0cb00218f

Cardoso-Avila, P. E., Patakfalvi, R., Rodríguez-Pedroza, C., Aparicio-Fernández, X., Loza-Cornejo, S., Villa-Cruz, V., & Martínez-Cano, E. (2021). One-pot green synthesis of gold and silver nanoparticles using: Rosa canina L. extract. *RSC Advances*, *11*(24), 14624–14631. https://doi.org/10.1039/d1ra01448j

Chowdhury, R., Khan, A., & Rashid, H. (2020). *Green synthesis of CuO nanoparticles using Lantana camara fl ower extract and their potential catalytic activity towards the aza-Michael reaction †*. 14374–14385. https://doi.org/10.1039/d0ra01479f

Cupido, M., De-Nova, A., Guerrero-González, M. L., Pérez-Vázquez, F. J., Méndez-Rodríguez, K. B., & Delgado-Sánchez, P. (2022). GC-MS analysis of phytochemical compounds of Opuntia megarrhiza (Cactaceae), an endangered plant of Mexico . *PeerJ Organic Chemistry*, *4*, e5. https://doi.org/10.7717/peerj-ochem.5

Datta, A., Patra, C., Bharadwaj, H., Kaur, S., Dimri, N., & Khajuria, R. (2017). *Journal of Biotechnology & Biomaterials Green Synthesis of Zinc Oxide Nanoparticles Using Parthenium hysterophorus Leaf Extract and Evaluation of their Antibacterial Properties*. *7*(3), 3–7. https://doi.org/10.4172/2155-952X.1000271

Dayana, S., Sc, K. M., Phil, M., Mani, J., Ph, R., Sc, D. N. M., D, V. S. P., Sophia, J., & Ph, P. (2021). *Biogenic synthesis of copper oxide nanoparticles using leaf extracts of Cissus quadrangularis and Piper betle and its antibacterial effects*. *January*, 1–6. https://doi.org/10.1049/mna2.12066

Demissie, M. G., Sabir, F. K., Edossa, G. D., & Gonfa, B. A. (2020). Synthesis of Zinc Oxide Nanoparticles Using Leaf Extract of Lippia adoensis (Koseret) and Evaluation of Its Antibacterial Activity. *Journal of Chemistry*, *2020*. https://doi.org/10.1155/2020/7459042

Devanesan, S., & AlSalhi, M. S. (2021). Green Synthesis of Silver Nanoparticles Using the Flower Extract of Abelmoschus esculentus for Cytotoxicity and Antimicrobial Studies. *International Journal of Nanomedicine*, *Volume 16*, 3343–3356. https://doi.org/10.2147/ijn.s307676

Dulta, K., Ko, G., Chauhan, P., Jasrotia, R., Chauhan, P. K., & Ighalo, J. O. (2022). *Multifunctional CuO nanoparticles with enhanced photocatalytic dye degradation and antibacterial activity*.

Dulta, K., Kosarsoy-agceli, G., & Jasrotia, R. (2022). *Ecofriendly Synthesis of Zinc Oxide Nanoparticles by Carica papaya Leaf Extract and Their Applications Ecofriendly Synthesis of Zinc Oxide Nanoparticles by Carica papaya Leaf Extract and Their Applications*. *March*. https://doi.org/10.1007/s10876-020-01962-w

El-belely, E. F., Farag, M. M. S., Said, H. A., Amin, A. S., Azab, E., & Gobouri, A. A. (2021). *Green Synthesis of Zinc Oxide Nanoparticles (ZnO-NPs) Using Arthrospira platensis (Class : Cyanophyceae) and Evaluation of their Biomedical Activities Green Synthesis of Zinc Oxide Nanoparticles (ZnO-NPs) Using Arthrospira platensis (Class : Cyanop*. *January*. https://doi.org/10.3390/nano11010095

El-Hawwary, S. S., Abd Almaksoud, H. M., Saber, F. R., Elimam, H., Sayed, A. M., El Raey, M. A., & Abdelmohsen, U. R. (2021). Green-synthesized zinc oxide nanoparticles, anti-Alzheimer potential and the metabolic profiling of Sabal blackburniana grown in Egypt supported by molecular modelling . *RSC Advances*, *11*(29), 18009–18025. https://doi.org/10.1039/d1ra01725j

Erci, F., Cakir-koc, R., Yontem, M., & Torlak, E. (2020). Synthesis of biologically active copper oxide nanoparticles as promising novel antibacterial- antibiofilm agents. *Preparative Biochemistry & Biotechnology*, *50*(6), 538–548. https://doi.org/10.1080/10826068.2019.1711393

Ezeonu, C. S., & Ejikeme, C. M. (2016). Qualitative and Quantitative Determination of Phytochemical Contents of Indigenous Nigerian Softwoods. *New Journal of Science*, *2016*, 1–9. https://doi.org/10.1155/2016/5601327

Faisal, S., Jan, H., Shah, S. A., Shah, S., Khan, A., Akbar, M. T., Rizwan, M., Jan, F., Wajidullah, Akhtar, N., Khattak, A., & Syed, S. (2021). Green Synthesis of Zinc Oxide (ZnO) Nanoparticles Using Aqueous Fruit Extracts of Myristica fragrans: Their Characterizations and Biological and Environmental Applications. *ACS Omega*, *6*(14), 9709–9722. https://doi.org/10.1021/acsomega.1c00310

Fouda, A., Salem, S. S., Wassel, A. R., Hamza, M. F., & Shaheen, T. I. (2020). Heliyon Optimization of green biosynthesized visible light active CuO / ZnO nano-photocatalysts for the degradation of organic methylene blue dye. *Heliyon*, *6*(July), e04896. https://doi.org/10.1016/j.heliyon.2020.e04896

Friday, A., Otalu, O., Ukwubile, C. A., & Onoruoyiza, O. V. (2020). Use of Medicinal Plants as Antimicrobial Agents: A Review of the Successes Story. *International Journal of Medicinal Plants and Natural Products*, *6*(3), 28–33. https://doi.org/10.20431/2454-7999.0603004

Garg, R. (2021). *Review article - A review on biogenic synthesis , applications and toxicity aspects of zinc oxide nanoparticles Review article : A REVIEW ON BIOGENIC SYNTHESIS , APPLICATIONS AND TOXICITY ASPECTS OF ZINC OXIDE NANOPARTICLES*. *September 2020*. https://doi.org/10.17179/excli2020-2842

Garibo, D., Borbón-Nuñez, H. A., de León, J. N. D., García Mendoza, E., Estrada, I., Toledano-Magaña, Y., Tiznado, H., Ovalle-Marroquin, M., Soto-Ramos, A. G., Blanco, A., Rodríguez, J. A., Romo, O. A., Chávez-Almazán, L. A., & Susarrey-Arce, A. (2020). Green synthesis of silver nanoparticles using Lysiloma acapulcensis exhibit high-antimicrobial activity. *Scientific Reports*, *10*(1), 1–11. https://doi.org/10.1038/s41598-020-69606-7

Gebremedhn, K., Kahsay, M. H., & Aklilu, M. (2019a). *Green Synthesis of CuO Nanoparticles Using Leaf Extract of*. *7*, 327–342. https://doi.org/10.17265/2328-2150/2019.06.007

Gebremedhn, K., Kahsay, M. H., & Aklilu, M. (2019b). *Green Synthesis of CuO Nanoparticles Using Leaf Extract of Catha edulis and Its Antibacterial Activity*. *7*, 327–342. https://doi.org/10.17265/2328-2150/2019.06.007

George, B. P., Houreld, N. N., & Abrahamse, H. (2021). *Synthesis of Zinc Oxide Nanoparticles Using Rubus fairholmianus Root Extract and Their Activity against*.

Ghamari Kargar, P., Noorian, M., Chamani, E., Bagherzade, G., & Kiani, Z. (2021). Synthesis, characterization and cytotoxicity evaluation of a novel magnetic nanocomposite with iron oxide deposited on cellulose nanofibers with nickel (Fe 3 O 4 @NFC@ONSM-Ni) . *RSC Advances*, *11*(28), 17413–17430. https://doi.org/10.1039/d1ra01256h

Gharby, A. (2021). *The Effect of Zinc oxide Nanoparticles (ZnO NPs) on the Viability of Leishmania tropica In Vitro The Effect of Zinc oxide Nanoparticles (ZnO NPs) on the Viability of Leishmania tropic In Vitro*. *January,* (2021).

Gilavand, F., Saki, R., Mirzaei, S. Z., Lashgarian, H. E., Karkhane, M., & Marzban, A. (2021). Green synthesis of zinc nanoparticles using aqueous extract of magnoliae officinalis and assessment of its bioactivity potentials. *Biointerface Research in Applied Chemistry*, *11*(1), 7765–7774. https://doi.org/10.33263/BRIAC111.77657774

Gonfa, T., Fisseha, A., & Thangamani, A. (2020). Isolation, characterization and drug-likeness analysis of bioactive compounds from stem bark of Warburgia ugandensis Sprague. *Chemical Data Collections*, *29*. https://doi.org/10.1016/j.cdc.2020.100535

Gulliford, M. C., Sun, X., Charlton, J., Winter, J. R., Bunce, C., Boiko, O., Fox, R., Little, P., Moore, M., Hay, A. D., & Ashworth, M. (2020). Serious bacterial infections and antibiotic prescribing in primary care: Cohort study using electronic health records in the UK. *BMJ Open*, *10*(2), 1–8. https://doi.org/10.1136/bmjopen-2020-036975

Gunathilaka, U. M. T. M., de Silva, W. A. P. P., Dunuweera, S. P., & Rajapakse, R. M. G. (2021). Effect of morphology on larvicidal activity of chemically synthesized zinc oxide nanoparticles against mosquito vectors. *RSC Advances*, *11*(15), 8857–8866. https://doi.org/10.1039/d1ra00014d

Han, Y., Han, Y., Du, G., Zhang, T., Guo, Q., Yang, H., Li, R., & Xu, Y. (2021). Physiological effect of colloidal carbon quantum dots onBursaphelenchus xylophilus. *RSC Advances*, *11*(11), 6212–6220. https://doi.org/10.1039/d0ra10144c

Hasan, I., & Singh, P. (2019). *Green Approach for Synthesis of Cuo Nanoparticles and their Application in Antimicrobial Activity*. 175–177. https://doi.org/10.19080/IJESNR.2019.17.555975

Hu, X. Le, Shang, Y., Yan, K. C., Sedgwick, A. C., Gan, H. Q., Chen, G. R., He, X. P., James, T. D., & Chen, D. (2021). Low-dimensional nanomaterials for antibacterial applications. *Journal of Materials Chemistry B*, *9*(17), 3640–3661. https://doi.org/10.1039/d1tb00033k

Huang, L., Zhu, X., Zhou, S., Cheng, Z., Shi, K., Zhang, C., & Shao, H. (2021). Phthalic acid esters: Natural sources and biological activities. *Toxins*, *13*(7). https://doi.org/10.3390/toxins13070495

Ifeanyichukwu, U. L., & Fayemi, O. E. (2020). *Green Synthesis of Zinc Oxide Nanoparticles from Pomegranate (Punica granatum) Extracts and Characterization of Their Antibacterial Activity*.

Ijaz, F., Shahid, S., Khan, S. A., & Ahmad, W. (2017). *Green synthesis of copper oxide nanoparticles using Abutilon indicum leaf extract : Antimicrobial , antioxidant and photocatalytic dye degradation activities*. *16*(April), 743–753.

Ikhioya, I. L., Nkele, C. A., & Obitte, B. (2023). *The The Green Synthesis of Copper Oxide Nanoparticles Using the Moringa Oleifera Plant and its Subsequent Characterization for Use in Energy Storage Applications*. *January*. https://doi.org/10.26565/2312-4334-2023-1-20

Infections, B. (2022). *An Annotated Inventory of Tanzanian Medicinal Plants Bacterial Infections*.

Irfan, M., Munir, H., & Ismail, H. (2021). Moringa oleifera gum based silver and zinc oxide nanoparticles: green synthesis, characterization and their antibacterial potential against MRSA. *Biomaterials Research*, *25*(1), 1–8. https://doi.org/10.1186/s40824-021-00219-5

Jan, H., Shah, M., Andleeb, A., Faisal, S., Khattak, A., Rizwan, M., Drouet, S., Hano, C., & Abbasi, B. H. (2021). *Plant-Based Synthesis of Zinc Oxide Nanoparticles (ZnO-NPs) Using Aqueous Leaf Extract of Aquilegia pubiflora : Their Antiproliferative Activity against HepG2 Cells Inducing Reactive Oxygen Species and Other In Vitro Properties*. *2021*.

Jayakodi, S. (2020). *Green Synthesis of CuO Nanoparticles and its Application on Toxicology Evaluation*. *10*(5), 6343–6353.

Jiang, S., Wang, M., Jiang, Z., Zafar, S., Xie, Q., Yang, Y., Liu, Y., Yuan, H., Jian, Y., & Wang, W. (2021). Chemistry and pharmacological activity of sesquiterpenoids from the chrysanthemum genus. *Molecules*, *26*(10). https://doi.org/10.3390/molecules26103038

Jiménez-Rodríguez, A., Sotelo, E., Martínez, L., Huttel, Y., González, M. U., Mayoral, A., García-Martín, J. M., Videa, M., & Cholula-Díaz, J. L. (2021). Green synthesis of starch-capped Cu2O nanocubes and their application in the direct electrochemical detection of glucose. *RSC Advances*, *11*(23), 13711–13721. https://doi.org/10.1039/d0ra10054d

Joshi, N. C. (2019). Leaves extract-based biogenic synthesis of cupric oxide nanoparticles , characterizations , and antimicrobial activity characterizations , and antimicrobial activity. *January*. https://doi.org/10.22159/ajpcr.2019.v12i8.34182

Joshi, N. C. (2020). *An eco-friendly synthesis of cupric oxide nanoparticles by using leaves extract of Psidium guajava , characterisations and antibacterial activities*. *8*(June), 38–41.

Journal, A. I., Hasheminya, S., & Dehghannya, J. (2020). Green synthesis and characterization of copper nanoparticles using Eryngium caucasicum Trautv aqueous extracts and its antioxidant and antimicrobial properties. *Particulate Science and Technology*, *38*(8), 1019–1026. https://doi.org/10.1080/02726351.2019.1658664

Kahsay, M. H., Tadesse, A., Ramadevi, D., Belachew, N., & Basavaiah, K. (2019). *RSC Advances*. *November*. https://doi.org/10.1039/C9RA07630A

Kalpana, V. N., & Devi Rajeswari, V. (2018). A Review on Green Synthesis, Biomedical Applications, and Toxicity Studies of ZnO NPs. *Bioinorganic Chemistry and Applications*, *2018*. https://doi.org/10.1155/2018/3569758

Karkhane, M., & Marzban, A. (2020). *Green Synthesis of Zinc Nanoparticles Using Aqueous Extract of Magnoliae Green Synthesis of Zinc Nanoparticles Using Aqueous Extract of Magnoliae officinalis and Assessment of its Bioactivity Potentials*. *July*. https://doi.org/10.33263/BRIAC111.77657774

Khan, S. A., Shahid, S., & Lee, C. S. (2020). Green synthesis of gold and silver nanoparticles using leaf extract of clerodendrum inerme; characterization, antimicrobial, and antioxidant activities. *Biomolecules*, *10*(6). https://doi.org/10.3390/biom10060835

Khanal, S. (2021). Qualitative and Quantitative Phytochemical Screening of Azadirachta indica Juss. Plant Parts. *International Journal of Applied Sciences and Biotechnology*, *9*(2), 122–127. https://doi.org/10.3126/ijasbt.v9i2.38050

Khatamifar, M., & Fatemi, S. J. (2021). Green synthesis of pure copper oxide nanoparticles using Quercus infectoria galls extract, thermal behavior and their antimicrobial effects. *Particulate Science and Technology*, *0*(0), 1–9. https://doi.org/10.1080/02726351.2021.1901810

Khodadadi, S., Mahdinezhad, N., Fazeli-Nasab, B., Heidari, M. J., Fakheri, B., & Miri, A. (2021). Investigating the Possibility of Green Synthesis of Silver Nanoparticles Using Vaccinium arctostaphlyos Extract and Evaluating Its Antibacterial Properties. *BioMed Research International*, *2021*, 1–13. https://doi.org/10.1155/2021/5572252

Kobylinska, N., Shakhovsky, A., Khainakova, O., Klymchuk, D., Avdeeva, L., Ratushnyak, Y., Duplij, V., & Matvieieva, N. (2020). "Hairy" root extracts as source for "green" synthesis of silver nanoparticles and medical applications. *RSC Advances*, *10*(65), 39434–39446. https://doi.org/10.1039/d0ra07784d

Kraus, C., Abou-Ammar, R., Schubert, A., & Fischer, M. (2021). Warburgia ugandensis leaf and bark extracts: An alternative to copper as fungicide against downy mildew in organic viticulture? *Plants*, *10*(12). https://doi.org/10.3390/plants10122765

Leonardi, M., Caruso, G. M., Carroccio, S. C., Boninelli, S., Curcuruto, G., Zimbone, M., Allegra, M., Torrisi, B., Ferlito, F., & Miritello, M. (2021). Smart nanocomposites of chitosan/alginate nanoparticles loaded with copper oxide as alternative nanofertilizers. *Environmental Science: Nano*, *8*(1), 174–187. https://doi.org/10.1039/d0en00797h

Lopez-miranda, J. L., Molina, G. A., Alexis, M., Liliana, B., Esparza, R., Silva, R., & Est, M. (2023). *Antibacterial and Anti-Inflammatory Properties of ZnO Nanoparticles Synthesized by a Green Method Using Sargassum Extracts*.

Maduabuchi, K., Xavier, E., Noundou, S., Maduelosi, B., & Nwachukwu, N. (2019). Green synthesis of zinc oxide nanoparticles using Solanum torvum (L) leaf extract and evaluation of the toxicological profile of the ZnO nanoparticles – hydrogel composite in Wistar albino rats. *International Nano Letters*, *9*(2), 99–107. https://doi.org/10.1007/s40089-018-0263-1

Mahalakshmi, S., Hema, N., & Vijaya, P. P. (2020). *In Vitro Biocompatibility and Antimicrobial activities of Zinc Oxide Nanoparticles (ZnO NPs) Prepared by Chemical and Green Synthetic Route — A Comparative Study*. 112–121.

Maina, M., Mwaniki, P., Odira, E., Kiko, N., McKnight, J., Schultsz, C., English, M., & Tosas-Auguet, O. (2020). Antibiotic use in Kenyan public hospitals: Prevalence, appropriateness and link to guideline availability. *International Journal of Infectious Diseases*, *99*, 10–18. https://doi.org/10.1016/j.ijid.2020.07.084

Makeswari, M. (2018). *Green synthesis , characterization and antibacterial studies of cuo nanoparticles from Eichhornia crassipes*. *July 2017*. https://doi.org/10.7324/RJC.2017.1031800

Mary, A. P. A., Ansari, A. T., & Subramanian, R. (2019). Journal of King Saud University – Science Sugarcane juice mediated synthesis of copper oxide nanoparticles , characterization and their antibacterial activity. *Journal of King Saud University - Science*, *31*(4), 1103–1114. https://doi.org/10.1016/j.jksus.2019.03.003

Midatharahalli, M., Shivayogeeswar, C., & Kotresh, E. N. (2019). Green synthesis of Zinc oxide nanoparticles (ZnO NPs) and their biological activity. *SN Applied Sciences*, *1*(1), 1–10. https://doi.org/10.1007/s42452-018-0095-7

Mohamed, E. A. (2020). Heliyon Green synthesis of copper & copper oxide nanoparticles using the extract of seedless dates. *Heliyon*, *6*(December 2019), e03123. https://doi.org/10.1016/j.heliyon.2019.e03123

Muhongo, M. N., Kangogo, M., & Bii, C. (2021). *Qualitative and quantitative phytochemical profiling of crude fractions of Pechuel-Loeschea leubnitziae leaves*. *15*(2), 64–72. https://doi.org/10.5897/JMPR2020.7073

Murthy, H. C. A., Desalegn, T., Kassa, M., Abebe, B., & Assefa, T. (2020). Synthesis of Green Copper Nanoparticles Using Medicinal Plant Hagenia abyssinica (Brace) JF. Gmel. Leaf Extract: Antimicrobial Properties. *Journal of Nanomaterials*, *2020*. https://doi.org/10.1155/2020/3924081

Muthukumaran, G. S. C., Santhiya, K. S. S., Pradeep, R. S., & Kumar, N. M. (2018). Biosynthesis , characterization , and antibacterial activity of zinc oxide nanoparticles derived from Bauhinia tomentosa leaf extract. *Journal of Nanostructure in Chemistry*, *0123456789*. https://doi.org/10.1007/s40097-018-0271-8

Mutukwa, D., & Taziwa, R. *A Review of the Green Synthesis of ZnO Nanoparticles Utilising Southern African Indigenous Medicinal Plants*, (2022).

Naga, P., Kumar, V., Shameem, P., Lakshmi, U., Ruddaraju, K., & Kollu, P. (2019). Antibacterial activity assessment and characterization of green synthesized CuO nano rods using Asparagus racemosus roots extract. *SN Applied Sciences*, *1*(5), 1–7. https://doi.org/10.1007/s42452-019-0449-9

Nagarajan, K. (2017). *Green Synthesis of Zinc Oxide Nanoparticles Using Fresh Stem of Cissus quadrangularis Extract and its Various in vitro Studies*. *April*. https://doi.org/10.14233/ajchem.2017.20483

Naseer, M., Aslam, U., Khalid, B., & Chen, B. (2020). Green route to synthesize Zinc Oxide Nanoparticles using leaf extracts of Cassia fistula and Melia azadarach and their antibacterial potential. *Scientific Reports*, *10*(1), 1–10. https://doi.org/10.1038/s41598-020-65949-3

Nie, Y. W., Li, Y., Luo, L., Zhang, C. Y., Fan, W., Gu, W. Y., Shi, K. R., Zhai, X. X., & Zhu, J. Y. (2021). Phytochemistry and pharmacological activities of the diterpenoids from the genus daphne. *Molecules*, *26*(21), 1–29. https://doi.org/10.3390/molecules26216598

Obakiro, S. B., Kiprop, A., Kigondu, E., K'owino, I., Kiyimba, K., Drago Kato, C., & Gavamukulya, Y. (2021). Sub-Acute Toxicity Effects of Methanolic Stem Bark Extract of Entada abyssinica on Biochemical, Haematological and Histopathological Parameters in Wistar Albino Rats. *Frontiers in Pharmacology*, *12*(September), 1–9. https://doi.org/10.3389/fphar.2021.740305

Obakiro, S. B., Kiprop, A., Kigondu, E., K'Owino, I., Odero, M. P., Manyim, S., Omara, T., Namukobe, J., Owor, R. O., Gavamukulya, Y., & Bunalema, L. (2021). Traditional Medicinal Uses, Phytoconstituents, Bioactivities, and Toxicities of Erythrina abyssinica Lam. ex DC. (Fabaceae): A Systematic Review. *Evidence-Based Complementary and Alternative Medicine*, *2021*. https://doi.org/10.1155/2021/5513484

Okello, D., & Kang, Y. (2021). Ethnopharmacological Potentials of Warburgia ugandensis on Antimicrobial Activities. *Chinese Journal of Integrative Medicine*, *27*(8), 633–640. https://doi.org/10.1007/s11655-019-3042-6

Olivia, N. U., Goodness, U. C., & Obinna, O. M. (2021). Phytochemical profiling and GC-MS analysis of aqueous methanol fraction of Hibiscus asper leaves. *Future Journal of Pharmaceutical Sciences*, *7*(1). https://doi.org/10.1186/s43094-021-00208-4

Pal, S., Mondal, S., Maity, J., & Mukherjee, R. (2018). Synthesis and characterization of zno nanoparticles using Moringa Oleifera leaf extract: Investigation of photocatalytic and antibacterial activity. *International Journal of Nanoscience and Nanotechnology*, *14*(2), 111–119.

Pathak, A., Upadhayay, R., Mathur, A., Rathi, S., & Lundborg, C. S. (2020). Incidence, clinical profile, and risk factors for serious bacterial infections in children hospitalized with fever in Ujjain, India. *BMC Infectious Diseases*, *20*(1), 1–11. https://doi.org/10.1186/s12879-020-4890-6

Pellico, J., Gawne, P. J., & T. M. De Rosales, R. (2021). Radiolabelling of nanomaterials for medical imaging and therapy. *Chemical Society Reviews*, *50*(5), 3355–3423. https://doi.org/10.1039/d0cs00384k

Perveen, R., Shujaat, S., Qureshi, Z., Nawaz, S., Khan, M. I., & Iqbal, M. (2020). Green versus sol-gel synthesis of ZnO nanoparticles and antimicrobial activity evaluation. *Integrative Medicine Research*, *9*(4), 7817–7827. https://doi.org/10.1016/j.jmrt.2020.05.004

Plucinski, A., Lyu, Z., & Schmidt, B. V. K. J. (2021). Polysaccharide nanoparticles: from fabrication to applications. *Journal of Materials Chemistry B*. https://doi.org/10.1039/d1tb00628b

Qamar, H., Rehman, S., Chauhan, D. K., Tiwari, A. K., & Upmanyu, V. (2020). *Green Synthesis , Characterization and Antimicrobial Activity of Copper Oxide Nanomaterial Derived from Momordica charantia*. 2541–2553.

Radhakrishnan, R., Liakath, F., Khan, A., & Muthu, A. (2021). *Green Synthesis of Copper Oxide Nanoparticles Mediated by Aqueous Leaf Extracts of Leucas aspera and Morinda tinctoria*. *10*(4), 2706–2714.

Rahman, F., Patwary, A. M., Siddique, A. B., Bashar, S., Haque, A., & Akter, B. (2022). *Green synthesis of zinc oxide nanoparticles using Cocos nucifera leaf extract : characterization , antimicrobial , antioxidant and photocatalytic activity*.

Ramzan, M., Obodo, R. M., Mukhtar, S., Ilyas, S. Z., Aziz, F., & Thovhogi, N. (2020). Materials Today : Proceedings Green synthesis of copper oxide nanoparticles using Cedrus deodara aqueous extract for antibacterial activity. *Materials Today: Proceedings*, *xxxx*. https://doi.org/10.1016/j.matpr.2020.05.472

Rangel, W. M., Boca Santa, R. A. A., & Riella, H. G. (2020). A facile method for synthesis of nanostructured copper (II) oxide by coprecipitation. *Journal of Materials Research and Technology*, *9*(1), 994–1004. https://doi.org/10.1016/j.jmrt.2019.11.039

Ravichandran, V., Sumitha, S., Ning, C. Y., Xian, O. Y., Yu, U. K., Paliwal, N., Adnan, S., Shah, A., & Tripathy, M. (2020). *Green Chemistry Letters and Reviews Durian waste mediated green synthesis of zinc oxide nanoparticles and evaluation of their antibacterial , antioxidant , cytotoxicity and photocatalytic activity*. https://doi.org/10.1080/17518253.2020.1738562

Roy M, A., Krishnan, L., & Roy Roy, A. (2018). Qualitative and Quantitative Phytochemical Analysis of Centella asiatica. *Natural Products Chemistry & Research*, *06*(04), 4–7. https://doi.org/10.4172/2329-6836.1000323

Sedlmeier, A., Gorris, H. H., Withers, P. J. A., Elser, J. J., Hilton, J., Ohtake, H., Schipper, W. J., Van Dijk, K. C., Kobylinska, N., Shakhovsky, A., Khainakova, O., Klymchuk, D., Avdeeva, L., Ratushnyak, Y., Duplij, V., Matvieieva, N., Yugandhar, P., Vasavi, T., Uma Maheswari Devi, P., … Matsabisa, M. G. (2020). The effect of ZnO particle lattice termination on the DC conductivity of LDPE nanocomposites. *RSC Advances*, *10*(1), 1–10. https://doi.org/10.1039/d0ra06858f

Selim, Y. A., Azb, M. A., Ragab, I., & El-azim, M. H. M. A. (2020). Green Synthesis of Zinc Oxide Nanoparticles Using Aqueous Extract of Deverra tortuosa and their Cytotoxic Activities. *Scientific Reports*, 1–9. https://doi.org/10.1038/s41598-020-60541-1

Selvakumar, S., Vimalanban, S., & Balakrishnan, G. (2019). Quantitative determination of phytochemical constituents from Anisomeles malabarica. *MOJ Bioequivalence & Bioavailability*, *6*(1), 19–21. https://doi.org/10.15406/mojbb.2019.06.00130

Sethuram, L., Thomas, J., Mukherjee, A., & Chandrasekaran, N. (2021). Eugenol micro-emulsion reinforced with silver nanocomposite electrospun mats for wound dressing strategies. *Materials Advances*, *2*(9), 2971–2988. https://doi.org/10.1039/d1ma00103e

Shaikh, J. R., Officer, L. D., Patil, M. K., & Udgir, A. S. (2020). *Qualitative tests for preliminary phytochemical screening : An overview Qualitative tests for preliminary phytochemical screening : An overview*. *August*. https://doi.org/10.22271/chemi.2020.v8.i2i.8834

Shammout, M. W., & Awwad, A. M. (2021). *A novel route for the synthesis of copper oxide nanoparticles using Bougainvillea plant flowers extract and antifungal activity evaluation*. 71–78.

Sharma, D., Thakur, N., Vashistt, J., & Bisht, G. S. (2018). *Antibacterial Evaluation of Cuprous Oxide Nanoparticles Synthesized Using Leaf Extract of Callistemon viminalis*. *52*(3), 449–455. https://doi.org/10.5530/ijper.52.3.52

Shi, Y., Xu, H., Liu, T., Zeb, S., Nie, Y., Zhao, Y., Qin, C., & Jiang, X. (2021). Advanced development of metal oxide nanomaterials for H 2 gas sensing applications . *Materials Advances*, *2*(5), 1530–1569. https://doi.org/10.1039/d0ma00880j

Shigwenya, E., Patrick, M., Kareru, G., Ngure, A., Mutuura, S., David, M., Makhanu, S., Indire, S., & Yahaya, W. (2020). Facile Synthesis of Silver Nanoparticles Using Lantana trifolia Aqueous Extracts and Their Antibacterial Activity. *Journal of Inorganic and Organometallic Polymers and Materials*, *0123456789*. https://doi.org/10.1007/s10904-019-01432-5

Singh, J., Kaur, S., Kaur, G., Basu, S., & Rawat, M. (2019). *Biogenic ZnO nanoparticles : a study of blueshift of optical band gap and photocatalytic degradation of reactive yellow 186 dye under direct sunlight*. 272–280.

Singh, P., Halder, M., Ray, S., Bose, A., & Sen, K. (2020). Green synthesis of silver and palladium nanocomposites: a study of catalytic activity towards etherification reaction. *Materials Advances, 1*(8), 2937–2952. https://doi.org/10.1039/d0ma00596g

Singh, P., Singh, K. R., Singh, J., Das, S. N., & Singh, R. P. (2021). Tunable electrochemistry and efficient antibacterial activity of plant-mediated copper oxide nanoparticles synthesized by Annona squamosa seed extract for agricultural utility. *RSC Advances*, *11*(29), 18050–18060. https://doi.org/10.1039/D1RA02382A

Siswadi, S., & Saragih, G. S. (2021). Phytochemical analysis of bioactive compounds in ethanolic extract of Sterculia quadrifida R.Br. *AIP Conference Proceedings*, *2353*(May). https://doi.org/10.1063/5.0053057

Soni, V., Jha, A. K., Dwivedi, J., & Dwivedi, P. S. (2018). Qualitative and quantitative determination of phytoconstituents in some antifertility herbs. *Indian Journal of Pharmaceutical Sciences*, *80*(1), 79–84. https://doi.org/10.4172/pharmaceutical-science.1000332

Sorbiun, M., Shayegan Mehr, E., Ramazani, A., & Mashhadi Malekzadeh, A. (2018). Biosynthesis of metallic nanoparticles using plant extracts and evaluation of their antibacterial properties ARTICLE INFO. *Nanochem Res*, *3*(1), 1–16. https://doi.org/10.22036/ncr.2018.01.001

Sousa De Almeida, M., Susnik, E., Drasler, B., Taladriz-Blanco, P., Petri-Fink, A., & Rothen-Rutishauser, B. (2021). Understanding nanoparticle endocytosis to improve targeting strategies in nanomedicine. *Chemical Society Reviews*, *50*(9), 5397–5434. https://doi.org/10.1039/d0cs01127d

Ssekatawa, K., Byarugaba, D. K., Angwe, M. K., Wampande, E. M., Ejobi, F., Nxumalo, E., Maaza, M., & Sackey, J. (2022). *Phyto-Mediated Copper Oxide Nanoparticles for Antibacterial , Antioxidant and Photocatalytic Performances*. *10*(February), 1–17. https://doi.org/10.3389/fbioe.2022.820218

Sutradhar, P., & Saha, M. (2016). Green synthesis of zinc oxide nanoparticles using tomato (Lycopersicon esculentum) extract and its photovoltaic application. *Journal of Experimental Nanoscience*, *11*(5), 314–327. https://doi.org/10.1080/17458080.2015.1059504

Sutradhar, P., Saha, M., & Maiti, D. (2014). *Microwave synthesis of copper oxide nanoparticles using tea leaf and coffee powder extracts and its antibacterial activity CuO*. 4–9. https://doi.org/10.1007/s40097-014-0086-1

T-thienprasert, N. P. (2022). *Plant Pathogenic Bacteria and Epidermoid Carcinoma Cells*.

Taherzadeh Soureshjani, P., Shadi, A., & Mohammadsaleh, F. (2021). Algae-mediated route to biogenic cuprous oxide nanoparticles and spindle-like CaCO3: a comparative study, facile synthesis, and biological properties. *RSC Advances*, *11*(18), 10599–10609. https://doi.org/10.1039/d1ra00187f

Tee, S. Y., & Ye, E. (2021). Recent advancements in coinage metal nanostructures and bio-applications. *Materials Advances, 2*(5), 1507–1529. https://doi.org/10.1039/d0ma00829j

Tucker, S., Autonomous, C., & Sundaranar, M. (2021). *Morinda citrifolia leaf extract mediated green synthesis of copper oxide nanoparticles and it ' s potential and antibacterial studies*. *14*(2), 897–904.

Ul-hamid, A., Dafalla, H., Hakeem, A. S., Haider, A., & Ikram, M. (2022). *In-Vitro Catalytic and Antibacterial Potential of Green Synthesized CuO Nanoparticles against Prevalent Multiple Drug Resistant Bovine Mastitogen Staphylococcus aureus*.

Umaru, I. J., Badruddin, F. A., & Umaru, H. A. (2019). Phytochemical Screening of Essential Oils and Antibacterial Activity and Antioxidant Properties of Barringtonia asiatica (L) Leaf Extract. *Biochemistry Research International*, *2019*. https://doi.org/10.1155/2019/7143989

Uyen, T., Thi, D., Nguyen, T., Thi, Y. D., & Ta, H. (2020). *Green synthesis of ZnO nanoparticles using orange fruit peel extract for antibacterial activities*. 23899–23907. https://doi.org/10.1039/d0ra04926c

Vanlalveni, C., Lallianrawna, S., Biswas, A., Selvaraj, M., Changmai, B., & Rokhum, S. L. (2021). Green synthesis of silver nanoparticles using plant extracts and their antimicrobial activities: a review of recent literature. *RSC Advances*, *11*(5), 2804–2837. https://doi.org/10.1039/d0ra09941d

Veeramani, V., Van Chi, N., Yang, Y. L., Hong Huong, N. T., Van Tran, T., Ahamad, T., Alshehri, S. M., & Wu, K. C. W. (2021). Decoration of silver nanoparticles on nitrogen-doped nanoporous carbon derived from zeolitic imidazole framework-8 (ZIF-8)via in situauto-reduction. *RSC Advances*, *11*(12), 6614–6619. https://doi.org/10.1039/d0ra10546e

Waris, A., Din, M., Ali, A., Ali, M., Afridi, S., Baset, A., & Ullah Khan, A. (2021). A comprehensive review of green synthesis of copper oxide nanoparticles and their diverse biomedical applications. *Inorganic Chemistry Communications*, *123*(October 2020), 108369. https://doi.org/10.1016/j.inoche.2020.108369

Yao, Y., Wang, D., Hu, J., & Yang, X. (2021). Tumor-targeting inorganic nanomaterials synthesized by living cells. *Nanoscale Advances*. https://doi.org/10.1039/d1na00155h

Zhang, Y., Li, M., Gao, H., Wang, B., Tongcheng, X., Gao, B., & Yu, L. L. (2019). *Triacylglycerol , fatty acid , and phytochemical profiles in a new red sorghum variety (Ji Liang No . 1) and its antioxidant and anti- - inflammatory properties*. *August 2018*, 1–10. https://doi.org/10.1002/fsn3.886

Zielińska-Błajet, M., & Feder-Kubis, J. (2020). Monoterpenes and their derivatives—recent development in biological and medical applications. *International Journal of Molecular Sciences*, *21*(19), 1–38. https://doi.org/10.3390/ijms21197078

Appendix I: Similarity Report

University of Eldoret

Certificate of Plagiarism Check for Synopsis

Author Name	Lemeitaron Peter Njenga SSCI/CHE/M/004/20
Course of Study	Type here...
Name of Guide	Type here...
Department	Type here...
Acceptable Maximum Limit	Type here...
Submitted By	titustoo@uoeld.ac.ke
Paper Title	BIOGENIC SYNTHESIS AND CHARACTERIZATION OF ZnO AND CuO NANOPARTICLES FROM Entada abyssinica AND Warburgia ugandensis LEAF EXTRACTS FOR ANTI-BACTERIAL APPLICATIONS
Similarity	12%
Paper ID	986385
Submission Date	2023-09-27 15:12:26

Signature of Student

Signature of Guide

Head of the Department

* This report has been generated by DrillBit Anti-Plagiarism Software